16ENG02   PV-Enerate

FINAL PUBLISHABLE REPORT

Grant Agreement number	16ENG02
Project short name	PV-Enerate
Project full title	Advanced PV Energy Rating

Project start date and duration:	01 May 2017, 41 months
Coordinator: Stefan Winter, Dr., PTB Tel: ++49 531 592-4500 E-mail: stefan.winter@ptb.de Project website address: http://www.pv-enerate.ptb.de/	

Internal Funded Partners:	External Funded Partners:	Unfunded Partner:
1 PTB, Germany 2 Aalto, Finland 3 INTA, Spain 4 LNE, France 5 NPL, United Kingdom 6 TUBITAK, Turkey	7 FhG, Germany 8 ISFH, Germany 9 JRC, Belgium 10 LU, United Kingdom 11 LUH, Germany 12 TÜV Rheinland, Germany	13 SUPSI, Switzerland
RMG1: IMBiH, Bosnia and Herzegovina (Employing organisation); PTB, Germany (Guestworking organisation)		

Final Publishable Report

TABLE OF CONTENTS

1   Overview

The project provided metrological infrastructure, techniques and guidance to accelerate time-to-market for emerging photovoltaics (PV) technologies, which have the potential to significantly reduce the cost of photovoltaic energy.

The project had two main objectives: Firstly, to improve the PV energy rating standards and secondly, to improve the measurement equipment and methodologies to enable precise measurements of the parameters required for the energy rating.

2   Need

According to the United Nations Framework Convention on Climate Change COP 21 in Paris, anthropogenic greenhouse gas emissions must be reduced drastically. As direct combustion of fossil fuels is reduced, renewable energy sources will cover the energy needs to the greatest extent – directly in individual sectors such as heating or in the form of renewable electricity, particularly from wind and solar energy. It is estimated that by 2050, electricity will cover roughly 50 % of all our energy needs – compared with around 25 % today. Renewable electricity will increasingly be used as an energy source and will primarily use technologies that replace a large amount of fuel with a small amount of renewable electricity. To minimise costs of energy storage, around one third of the renewable energy will be produced by photovoltaics.

Currently PV modules are optimised, selected and sold on the basis of power produced under standard test conditions (STC), however this does not allow for differentiation according to the most relevant parameter in the marketplace which is energy production under specific climatic conditions. However, this metric does not always reflect real-world conditions as location-dependent variations in ambient temperature, irradiance, angle-of-incidence, spectrum and wind-speed cause deviations in annually averaged module efficiencies of up to 20 %. This impedes the uptake of emerging and innovative technologies, such as modules optimised for specific climates.

A new set of standards, IEC 61853 provides a framework for energy rating of PV, including measurement, modelling and reference meteorological data. This is an important first step towards universal energy rating of PV modules, however, stakeholders have identified a number of remaining challenges arising from emerging technologies and market trends:

- Bifacial modules claim to increase energy yields by 10 % - 20 % by harvesting light from the rear of the panel, yet investors are nervous about the lack of standard tests and rating methods,

- PV modules on buildings experience different operating conditions compared to ground-mounted PV and this is not reflected in the current documentary standards,

- Module characterisation requires the use of new technology (such as LED simulators) for fast and accurate characterisation at the module scale and to harmonise handling of test data in order to improve the uptake of energy rating,

Thus, precise metrology and realistic, representative standards for PV are required to support one of the most important future energy sources.

3   Objectives

The project extended the metric for an energy-based photovoltaic classification to roof-mounted photovoltaics as well as to the fast-growing fields of bifacial and building-integrated photovoltaics.

The specific objectives of the project were:

1. To define and realise standard testing conditions for the measurement of the power or the short-circuit current of bifacial solar devices Different approaches for laboratory measurements and for production line measurements will be developed, realised, compared, selected and standardised. This will form the basis for the extended energy rating and the standardisation of measurement of bifacial solar devices.

2. To improve the method of uncertainty evaluation of the spectral mismatch correction in the calibration of solar devices when combining the spectral irradiance and spectral responsivity, taking the correlation of the spectral data into account.

3. To develop traceable measurement methods for extending energy rating to bifacial solar modules and to modules (bifacial or monofacial) applied to or integrated into buildings. This will include the definition of a harmonised data format for solar device properties, required for PV Energy rating measurement standards.

4. To enable instantaneous measurement of the spectral radiance of the complete sky for improved determination of real outdoor measurement conditions and the irradiance spectral-angular distribution by hyperspectral imaging.

5. To develop more accurate measurement methods for traditional and emerging solar modules, including the spectral responsivity of the complete module, fast linearity measurements for modules, angular dependency of modules, with an uncertainty of <1 % for the angular dependency impact, <3 °C for the nominal operating module temperature (NOMT), <1 % for the impact of spectral responsivity and <1 % for the impact of non-linearity.

6. To facilitate the uptake of the technology and measurement infrastructure developed in the project by the measurement supply chain (NMIs, calibration laboratories), standards developing organisations and end users (photovoltaics industry).

4   Results

To define and realise standard testing conditions for the measurement of the power or the short-circuit current of bifacial solar devices Different approaches for laboratory measurements and for production line measurements will be developed, realised, compared, selected and standardised. This will form the basis for the extended energy rating and the standardisation of measurement of bifacial solar devices (Objective 1):

Definition and realisation of standard test conditions for the measurement of bifacial solar devices

The aim of this objective has been to define and realise standard testing conditions (STCs) for bifacial solar devices in order to determine precisely their current-voltage characteristics.

The precise measurement of the illuminated current-voltage characteristics is of central importance for solar cell and module manufacturers. While the procedure and standard testing conditions for the measurement of conventional monofacial solar devices is well established and defined in standard IEC 60904-1, there is currently no general consensus on the measurement of bifacial solar devices since the IEC 60904-1 does not account for bifaciality. The most intuitive strategy for the measurement of bifacial solar devices is oriented towards the operation of the solar devices in field and includes the illumination of the device from both the front and the rear during measurements. While the front intensity is defined in common monofacial standard testing conditions, the rear intensity needs to be reduced to represent the intensity losses resulting from non-ideal ground reflectance onto the rear of the device.

Literature review and stakeholder analysis of the requirements for measurements of bifacial solar devices

A literature review regarding procedures and setups for measuring bifacial solar devices has been jointly carried out by FhG, PTB and University of Aalto. These procedures and setups are either based on both-sided illumination of the bifacial device or on front-side illumination only. Current-voltage (*I-V*) measurements are performed both outdoors and indoors.

For outdoor measurements, natural sunlight is used to illuminate the front and the rear side of the bifacial solar device. The rear irradiance is thereby varied by modifying the ground coverage with different reflectivities.

For indoor measurements, different types of solar simulator setups exist. The both-sided illumination is thereby either realized by two independent light sources or by one single light source and two mirrors deflecting light to the front and rear. Measurements under single-sided illumination are generally carried out indoors. Solar

simulators are operated at irradiances higher than standard testing conditions in order to account for additional current that would be generated by illumination of the rear side. This method is generally referred to as equivalent irradiance (G_E) method.

For the G_E method, the bifaciality coefficients φ_{Isc} and φ_{Pmpp} are initially calculated from the ratios of rear to front short-circuit current and maximum power, respectively, which need to be determined at STC:

$$\varphi_{Isc} = \frac{I_{sc,rear}}{I_{sc,front}} , \qquad \varphi_{Pmpp} = \frac{P_{mpp,rear}}{P_{mpp,front}} .$$

It is important that a non-reflective cover or measurement chuck is applied for the measurement to minimize contributions of transmitted and reabsorbed light. To account for the additional power that would be generated by rear side illumination, the front irradiance is increased to above 1000 W/m^2. This means that additional front side I-V measurements need to be performed with equivalent irradiance levels

$$G_E = 1000 \text{ Wm}^{-2} + \varphi \cdot G_{rear} \qquad \text{with} \qquad \varphi = \min(\varphi_{Isc}, \varphi_{Pmpp}).$$

φ thereby is equal to the minimum of φ_{Isc} and φ_{Pmpp} and serves as weight for the rear irradiance G_{rear}. These measurement procedures have been summarized in the IEC technical specification (TS) 60904-1-2, which has been published in 2019 with the collaboration of the PV-Enerate consortium. The compatibility of these procedures has not been clarified conclusively in the literature nor in the IEC TS and has been investigated in more detail in this project.

To identify the key aspects for further improvements as assessed by stakeholders of bifacial measurements. a questionnaire was designed by FhG and distributed among stakeholders. The completed questionnaires sent back to the consortium were thoroughly evaluated. The evaluation showed that indoor measurements with single-sided illumination at STC are current industry standard. More advanced methods are only applied by parts of the stakeholders, mainly using the G_E method. Thereby, a rear irradiance of 200 W/m^2 is standardly used for determining G_E. Nearly all sun simulators can be applied at irradiance levels higher than 1000 W/m^2, which makes measurements at elevated irradiance levels feasible at low effort. Although not being current industry standard, measurements with both-sided illumination are performed by four stakeholders, all of them equipment suppliers. For further improvement of the measurement procedures, high measurement accuracy, the usage of single-sided illumination and the applicability for energy rating and bifacial gain calculations were rated as the most important aspects.

It is interesting to note that solar device producers and equipment manufacturers offering inline systems rated high throughput as key aspect, whereas research institutes estimate throughput as irrelevant. This indicates that there are different requirements for production line environments and for calibration laboratories, which could potentially be resolved by the development of two different measurement approaches. Measurement accuracy should thereby always be kept in mind, which was considered as the most important aspect of all.

Improvement of the measurement setups and hardware for measuring the characteristics of bifacial solar devices

Aalto, FhG, INTA, ISFH, JRC, LU and PTB have comprehensively upgraded their facilities for the measurement of bifacial solar cells and modules.

University of Aalto has upgraded their LED-based differential spectral responsivity setup to cover the wavelength range of 290 nm – 1300 nm by introducing three new UV LEDs and characterizing all LEDs. Two new bias light towers were assembled behind the solar cell to enable spectral response measurements of bifacial solar cells (see Figure 1). A second approach for providing the rear bias light with a reflecting material sheet was also investigated. A new mechanical assembly to attach bifacial cells was built. Aalto has written a publication on the development of the setup and on DSR measurements of bifacial cells [Opt. Rev., https://doi.org/10.1007/s10043-020-00584-x].
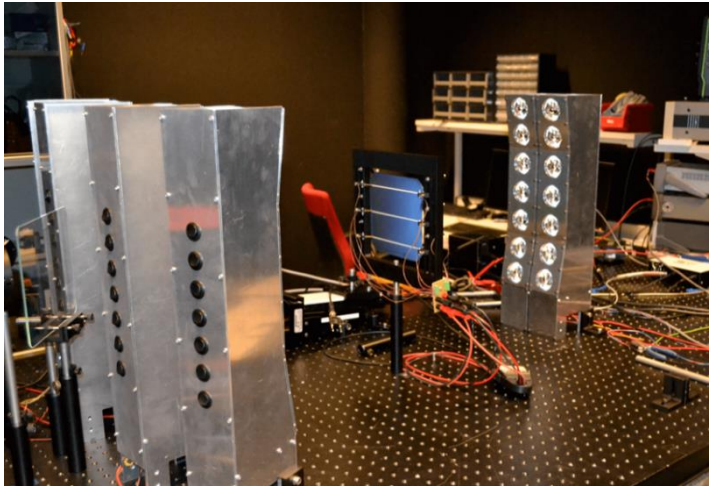
Figure 1: Upgrades of the Aalto spectral response setup. A bifacial solar cell has been assembled into the new cell holder. Two additional lamp towers have been assembled to illuminate the rear side of the cell.

To realize *I-V* measurements of bifacial solar cells with single- and both-sided illumination, a setup with one light source and two mirrors has been developed by FhG. The cell is placed vertically between two tilted mirrors, which reflect light of a xenon flash lamp to the front and rear sides of the cell (see Figure 2). For one-sided illumination, only the front light path is opened. For both-sided illumination, both light paths are used.
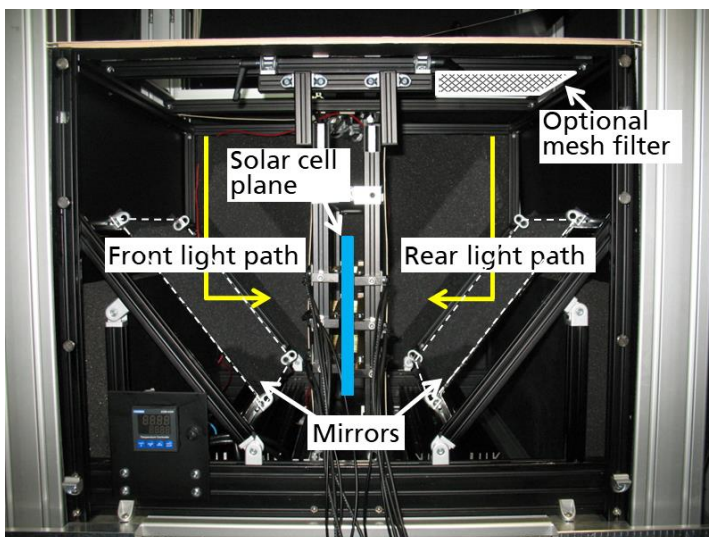

Figure 2: Front view image of the two-mirror setup used at FhG for measuring the *I-V* characteristics of bifacial solar cells with single- and both-sided illumination (front lid opened).

Figure 55 The accuracy of the setup has been thoroughly improved. A class-A spectrum of the front and rear illumination was ensured by adapting the spectral filters in front of the flash lamp. The uniformity of the front and rear irradiance in the solar cell plane was measured to be better than classification A (1.2 % for the front side and 1.1 % for the rear side at 1000 W/m^2). To furthermore prevent light from passing from one side to the other side of the solar cell, non-reflective, moveable apertures were installed, which can be moved very close to the edges of the solar cell from all sides. A temperature regulation unit and an isolating enclosure are used to stabilize the temperature of the bifacial solar cell to 25.0 ± 0.3°C. Calibrated tactile Pt100 sensors have been installed on a central busbar in a non-destructive way to track the solar cell temperature during measurements. Different approaches for the calibration of rear irradiance have been evaluated and the procedure with lowest measurement uncertainty identified and established.

The measurement uncertainties for the *I-V* parameters of both bifacial and equivalent irradiance methods have been determined by means of Monte Carlo simulations taking into account correlations between the different contributions. As both measurements are applied at the same setup, the difference between the two methods

can be measured with high precision because significant contributions to the measurement uncertainty cancel out. The difference in I_{sc} and P_{mpp} can be measured with expanded uncertainties in the range of 0.24 to 0.36 % and 0.53 to 0.59 %, respectively, for the configurations specified by IEC TS 60904-1-2.

ISFH has developed a bifacial measurement chuck for local rear contacting of solar cells with 5 busbars. Different coloured (black, white and gold) plates are available. Test measurements show a good reproducibility of the fill factor. Also, a good consistency is achieved to another bifacial chuck. In addition, a black locally contacting measuring block and a highly reflective measuring block with a glued-in sense segment have been put into operation. While the black measuring block was specially developed for solar cells with 5 busbars, solar cells with any number of busbars can be contacted on the highly reflective measuring block. IV measurements were carried out using either a local sense contacting with a spring-loaded contacting probe or a sensing segment inserted into the measurement chuck. Both sensing types yield equal characteristic solar cell parameters.

The ESTI existing facilities were upgraded and adapted for the measurements of bifacial PV modules according to the IEC TS 60904-1-2 using the single-side illumination method and the equivalent irradiance approach. This method may use either the Pasan III or the Apollo steady-state simulator. This led to the accreditation of the ESTI lab under the ISO17025 for the calibration of bifacial modules. Double-side illumination approaches were also tested, such as the use of a white reflective material placed behind the module or additional rear-side bias light based on LEDs (see Figure 3).
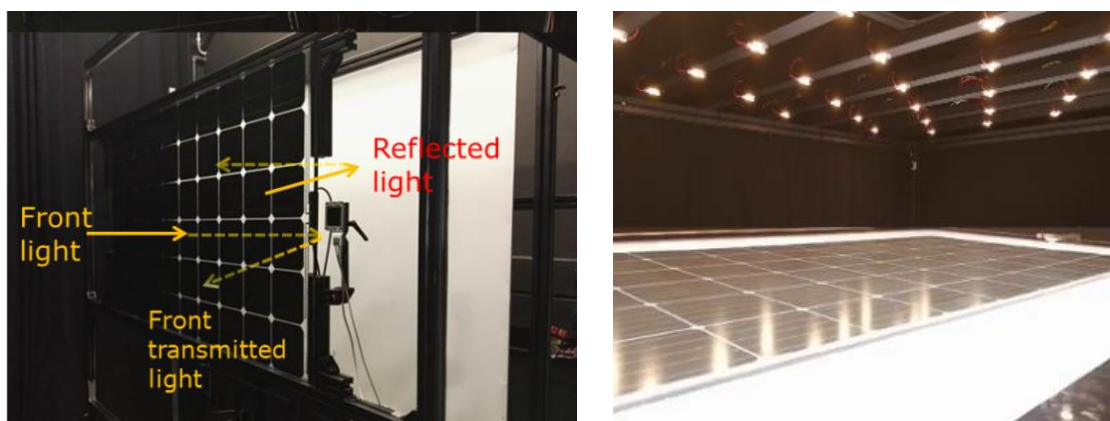

Figure 3: Setups at ESTI for double-side illumination with white rear reflector (*left*) and with LED-based bias light (*right*).

PTB has developed a solar cell holder that allows the two side illumination of bifacial solar cell (see Figure 4). This holder was constructed by a solid frame with 20 freely adjustable Kelvin probes for front and rear side contacting. Pt100 temperature sensors measure the solar cell temperature at the top and bottom edge of the solar cell. Since the DSR-facility at PTB utilized halogen lamps to generate the 1000 W/m² bias irradiance, the cooling of the solar cell is of crucial importance. The cooling was realized by a temperature stabilized air cooling from the side.
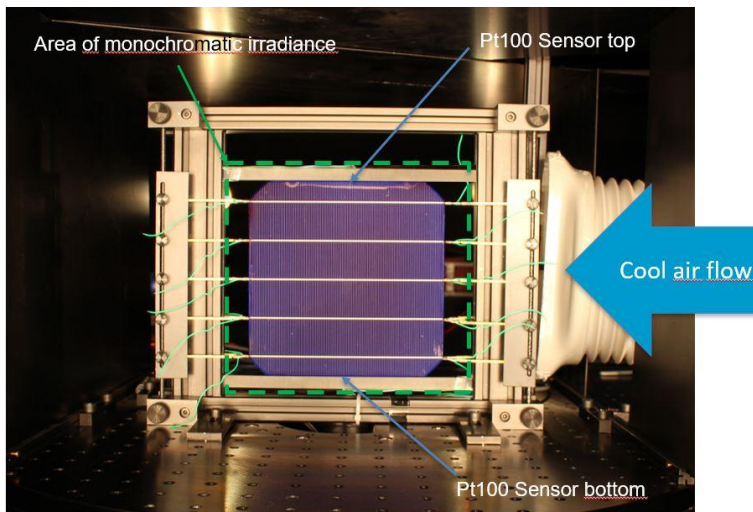
Figure 4: Measurement chuck of a free-floating solar cell for simultaneous illumination from front and rear side at PTB.

Development and evaluation of laboratory and production line measurement procedures for bifacial solar devices

As it has not been clarified before this project whether nonlinearity of bifacial solar cells is critical in terms of consistency of the measurement methods, ISFH has determined the linearity of several bifacial solar cells using their DSR facility. The monofacial cells (nPERT, nP048-11) showed a non-linearity (NL) of 0.2%. In contrast, the provided bifacial cells showed a higher NL value of 0.4% (front side, FS) and 0.9% (rear side, RS) for the nPERT cells and 0.6% (FS) and 3.5% (RS) for the PERC cells. Figure 5 shows the non-linearity of the different cells as a function of irradiance.
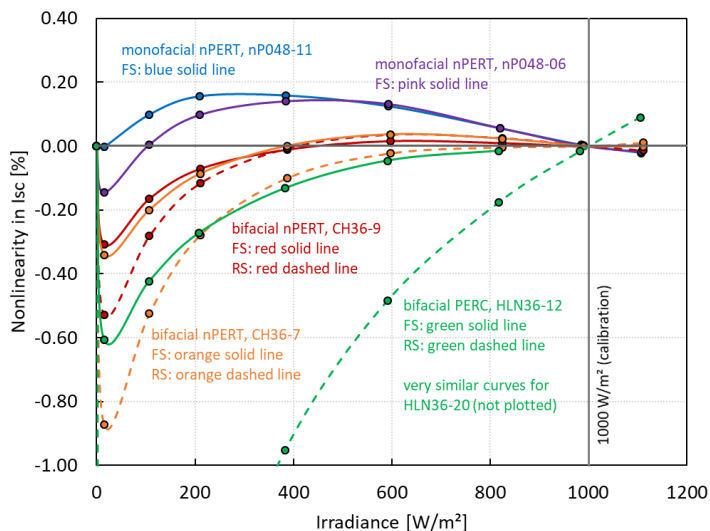

Figure 5: Non-linearity of different monofacial and bifacial solar cells as a function of irradiance measured with the DSR facility at ISFH.

FhG has measured the *I-V* characteristics of solar cells of various technology, including also bifacial passivated emitter and rear (PERC) cells with very strong nonlinearity, with the two-mirror setup of Figure 2. Differences in *I-V* parameters between the method comprising both-sided illumination and the G_E method were measured to be below 0.1 %$_{rel}$, which is clearly within the corresponding measurement uncertainties. The two methods can therefore indeed be considered as consistent on solar cell level, also for bifacial solar cells with strong nonlinearity.

For bifacial modules though, it has been shown by FhG that differences between the measurement methods with both-sided illumination and front illumination with elevated intensity can occur.

Current mismatch and partial rear shading can lead to deformation and kinks in the rear *I-V* curves of the bifacial modules, which reduce the maximum power point under rear illumination and lead to a difference between φ_{Isc} and φ_{Pmpp}. This difference has been measured to range up to more than 10 %$_{abs}$ for modules not optimized for bifacial applications. Whereas rear kinks thus strongly affect the input parameters for the G_E method according to the IEC TS (which applies the minimum of φ_{Isc} and φ_{Pmpp}), the impact on the method with both-sided illumination is significantly less strong: The maximum power point (mpp) of the *I-V* curve measured with both-sided illumination is often not affected by the kinks as the rear contribution is superimposed by the much stronger front contribution.

FhG has shown that following the IEC procedures for modules not optimized for bifacial applications can lead to errors in *BiFi* of more than 18 % and to errors in $P_{mppBiFi20}$ of more than 2 % (N.B: *BiFi* and $P_{mppBiFi20}$ are standardized measures for the power gain of the bifacial device caused by additional rear irradiance), by comparing measurements with the G_E method and the method comprising both-sided illumination (see Figure 6). The agreement of the results can be considerably improved to 1.1 % and 0.1 %, respectively when φ_{Isc} is used for the determination of G_E.

FhG has furthermore investigated the applicability of the G_E method using φ_{Isc} only by systematically varying the rear shading of two bifacial modules. It is shown that good agreement to the method with both-sided illumination is achieved as long as the contribution of the rear shading does not affect the mpp of the both-sided method. This is only the case for extensive rear shading or high rear irradiance levels. A criterion has been introduced to assess the applicability of the G_E method on the front and rear *I-V* curves measured at STC. For the irradiance conditions specified by the IEC TS, all typical module designs should meet the criterion and the G_E method using φ_{Isc} can be versatilely applied. Deviations may occur for solar modules intended for vertical east-west installation, which are not yet covered by the IEC TS though.

It is therefore suggested to omit the minimum criterion and to only use φ_{Isc}, which is also physically more meaningful. It is shown that the both-sided and the G_E methods can then be applied in good accordance.
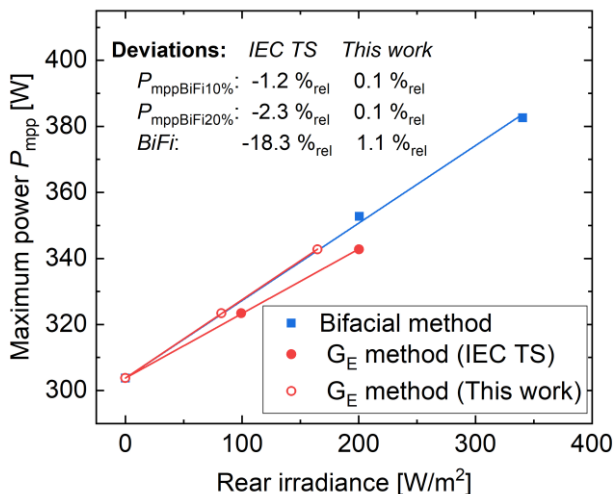

Figure 6: Maximum power P_{mpp} measured by FhG for different rear irradiance levels with both-sided illumination (blue squares) or with front-side illumination only using the G_E method (orange circles). The deviations in the standardized parameters $P_{mppBiFi10}$, $P_{mppBiFi20}$ and *BiFi* between the G_E method and method with both-sided illumination are given in the table in the figure.

ESTI at JRC has tested several different bifacial modules in their indoor and outdoor setups. With the indoor setup with a white rear reflector, high irradiance levels were obtained but with a high non-uniformity of the rear irradiance (above the permissible limit set by the IEC TS 60904-1-2). The use of LEDs as bias light increased the rear-side illumination to the required values (0-300 W/m^2) within the rear-irradiance non-uniformity requirement but further experiments are needed in order to solve spectral match and mismatch factor issues between both simulators. Improvements might be possible with different white reflective materials close to

Lambertian surfaces, and implementation of spectral mismatch corrections for LED bias light double-side illumination approach.

Characterisation of bifacial PV modules in real outdoor conditions was also tested (Figure 7 (a)). It was shown that the control of the measurement conditions as requested by the TS is difficult and strongly depends on the ground material. The G_{rear} determination and G_{rear} non-uniformity also had a significant impact on parameters that need to be reported, such as *BiFi*, $P_{maxBiFi10}$ and $P_{maxBiFi20}$ in outdoor characterisation. In general, a significant difference between indoor and outdoor results was obtained even if both methods are applied as proposed by the TS indicating that the indoor method is more reproducible and controllable to determinate *BiFi* and the $P_{maxBiFi}$ values (Figure 7 (b)).
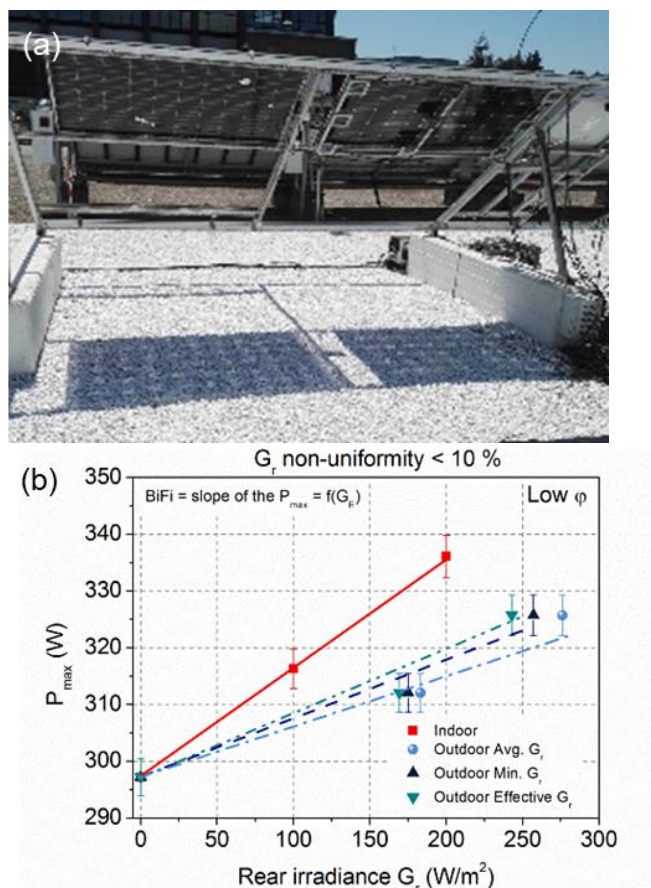

Figure 7:.(a) Setup at JRC for outdoor measurements with white reflective gravel on ground. (b) Maximum power measured indoors and outdoors as a function of rear irradiance.

In conclusion, the suitability of the outdoor approach for the characterisation of bifacial PV modules under the current requirements of the IEC TS 60904-1-2 seems to be low in comparison with the indoor methods.

Intercomparison of measurements of bifacial solar devices by the partners

An intercomparison activity for bifacial solar cells and modules has been jointly organized by NPL and the participating partners. Three batches of bifacial solar cells with different rear contacting schemes were produced by ISFH and a set of 12 bifacial modules has been purchased. Monofacial devices, which were included for reference purposes, have been taken from existing stocks.

A measurement protocol which was based on the optimal procedures derived in this objective for laboratory and production environments and on the IEC TS 60904-1-2 has been set up by NPL. The activity involved measurements with systems using both single and double-sided illumination conditions. NPL analysed all results from the partners.

Measurements of bifacial PV cells have demonstrated that, while consistent results are acquired, further improvements on the IEC technical specification should be considered. A better procedure for determining the background (rear side) irradiance, such as *e.g.* requirements for the spectral reflectivity of the testing platform,

when applying the equivalent irradiance (G_E) method for bifacial PV cells are required and can help towards decreasing uncertainties. No specific differences between the double-sided illumination measurements and the G_E method with single-sided illumination were observed for the bifacial PV cells of the round robin.

Measurements of bifacial PV modules based on the standard procedures produced consistent results among the different partners, with deviations for most measured and calculated parameters being within the uncertainty budgets provided by some of the partners (see Figure 8). Deviations for the front side are consistently lower than for the rear side, which can be attributed to measurement system differences at each lab (such as mounting configurations), the level of background rear-side irradiance or spectral mismatches. The highest deviations for all parameters are observed for *BiFi*, without however causing significant deviations in the values of $P_{maxBiFi10}$ and $P_{maxBiFi20}$. This highlights that higher deviations can be expected and the uncertainty budget for *BiFi* should always be considered.
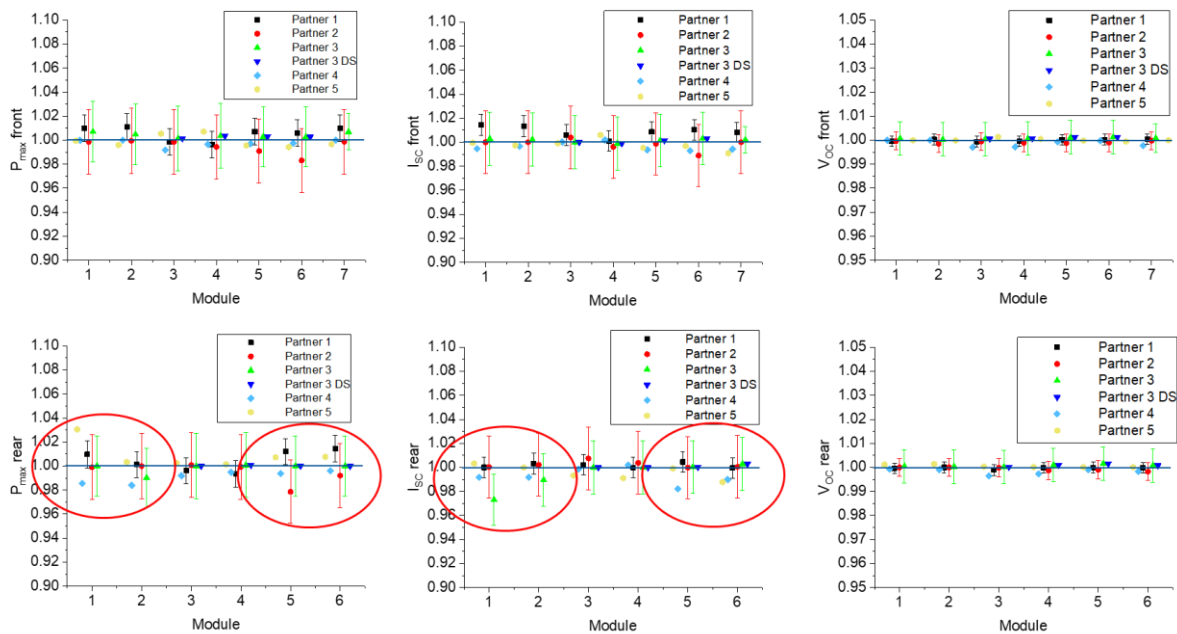

Figure 8: I_{SC}, P_{max} and V_{OC} for the front side (top row) and rear side (bottom row) of the bifacial PV modules, measured by different partners. Values are normalised by the median value. Module 7 is monofacial. The measurements with a double-sided system are marked as "DS".

The results have demonstrated that the observed deviations occurred mostly for the rear side of PV modules that feature differences in the spectral responsivity of front and rear side, or have a much larger size than usual. This demonstrates that the spectral responsivity of both sides of a bifacial PV module has to be considered in spectral mismatch calculations. Modules 3 and 4, for example, are modules built from hetero junction cells with high bifaciality factors and a small difference in spectral responsivity between the front and rear side. This is likely the reason why lower deviations can be observed for the rear side I_{SC} and P_{max} values for these modules, compared to the other two types of modules.

These small deviations also affect the calculation of the bifaciality coefficient φ. The measurements of the bifacial parameters *BiFi* and $P_{maxBiFi20}$ are summarized in Figure 9. These were determined from linear fits to P_{max} as function of the actual or compensated rear irradiance G_{rear}. The deviations for φ are in most cases within the uncertainty budgets provided by some of the partners. While there are apparent differences in the measurement of the *BiFi* parameter, they fall within the uncertainty budgets. $P_{maxBiFi10}$ (not shown) and $P_{maxBiFi20}$ parameters present the same deviations between the partners as the P_{max} values. There is a negligible difference between the single- and double-sided systems for the partner that has used both systems.
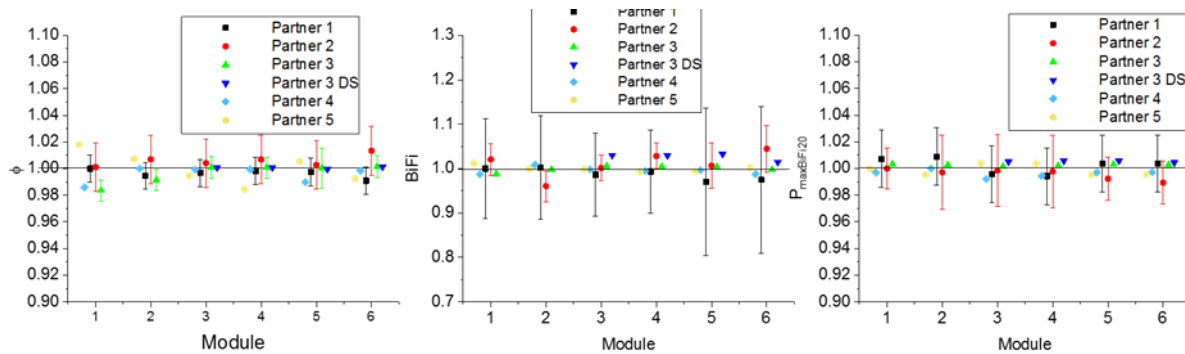
Figure 9: Bifacial coefficient φ as well as bifacial parameters *BiFi* and $P_{maxBiFi20}$ measured by different partners of the bifacial PV module round robin. Values are normalised by the median value. The measurements with a double-sided system are marked as "DS".

It was identified that the IEC technical specification is not concise in how to correctly apply the equivalent irradiance method to determine the power gain caused by additional rear irradiance. The linear fit of P_{max} needs to be evaluated as a function of G_{rear} and not as a function of G_E. In the latter case, several difficulties arise: The linear fit needs to be set to P_{max} measured at STC in an iterative way. Additionally, the slope of the linear fit needs to be divided by φ to derive *BiFi*.

In several occasions, measurement differences between laboratories that were identified in the course of the round robins led to improvements of measurement setups for some partners. One partner for example significantly improved the accuracy of their bifacial cell measurements through technical meetings and advises from other partners, when significant deviations with other partners were identified. A complete redesign of the contacting system was strived for.

The results of the round robin activities were presented at the EU PVSEC 2020 to a broad audience by NPL. Further consideration of the results were ensured by passing recommendations for improvements on the IEC TS 60904-1-2 procedures to technical committee 82 of working group 2. The round robin activity drew significant interest from the European PV community and additional external participants asked to participate in the activity, subsequent to the participation of the main partners of the project. This increased the impact of the round robin activity, but also extended the timeline of the activity outside the duration of the PV-Enerate project for the additional partners.

Impact

The consortium has continuously contributed to the development of the IEC technical specification 60904-1-2, which has been published in 2019, by giving general, editorial and technical comments as well as by checking the different versions of the document.

Several recommendations have been submitted, mainly within discussions during the meetings of IEC technical committee (TC) 82 of working group 2 and incorporated in the technical specification. The main issues pushed by the PV-Enerate consortium are the addition of a two light source method (illumination of front side and back side) that can be used in addition to the previously favoured one light source method with increased light power. The two light-source method represents more realistic test conditions and does not need overpowering of the light source for the front side. The second issue pushed by the consortium is the application of different background colours (grey and as black as possible) to enable an extrapolation to completely black background without interreflections.

Further recommendations and amendment proposals, that have been developed within this project after the publication of the technical specification, have been summarized by JRC in a report and submitted to the convenor of TC 82 in order to improve the approaches and procedures for characterisation of bifacial devices further.

The main proposed amendments focused on improvements and clarification of the rear irradiance and non-reflective material conditions (*i.e.* suitable distance from module to non-irradiated background). It has also been proposed to modify the determination of the bifaciality: Only the short-circuit bifaciality coefficient φ_{Isc} should be considered for the calculation of the equivalent irradiance. Moreover, it has been recommended to clarify the calculation of the *BiFi* parameter: It should be clear and highlighted that the G_{rear} data series is used for the calculation and not the G_E data series.

These amendments will help to improve and clarify the TS to avoid misunderstandings and will also contribute to the confidence of manufacturers and customer and the support and development of the bifacial PV market.

FhG, Aalto, INTA, LNE, NPL, PTB, ISFH, JRC, LU and SUPSI worked for this objective that resulted in deliverable D1. For the success of this objective it was required to test and compare different approaches. As different partners focussed on different methods, this objective could not have successful if it would be done by only one individual partner.

Several recommendations for the measurement of bifacial solar devices have been submitted, mainly within discussions during the IEC TC82-WG2 meetings. The main issues being recommended by members of the PV-Enerate consortium are use of different background colours (grey and as black as possible) to enable an extrapolation to completely black background without interreflections. The second issue put forward by the consortium is the addition of a two light-source method (illumination of front side and back side) that can be used in addition to the previously favoured one light source method with increased light power. The two light-source method realizes more realistic test conditions and does not need overpowering of the light source for the front side. The IEC TS 60904-1-2 "Photovoltaic devices - Part 1-2: Measurement of current-voltage characteristics of bifacial photovoltaic (PV) devices" was published as a technical specification at 2019-01-29. Many new installations are using the two light-source method propagated by the project team. Within the project a comparison between different members of the consortium and stakeholders / collaborators were successfully performed. This objective was successfully achieved.

To improve the method of uncertainty evaluation of the spectral mismatch correction in the calibration of solar devices when combining the spectral irradiance and spectral responsivity, taking the correlation of the spectral data into account (Objective 2):

Improvement of the method of uncertainty evaluation of the spectral mismatch correction

The aim of this objective is to improve the uncertainty evaluation of the spectral mismatch correction, which is one of the largest uncertainty components associated with the calibration of solar devices using solar simulators.

The influence of the numerical calculation methodology, i.e. the influence of (i) the mathematical function used for the interpolation of the spectral responsivities and of (ii) the numerical integration of products of spectral responsivity and spectral irradiance on the spectral mismatch and its uncertainty, on the mismatch uncertainty will be assessed. At least 10 different spectral responsivities and spectral irradiances with different spectral resolutions will be used to evaluate the calculation methods. Different methods for combining the uncertainties of the spectral responsivity and the spectral irradiance respectively into the spectral mismatch uncertainty will be evaluated.

The influence of a) interpolation and b) different numerical tools on the calculation of the spectral mismatch (SMM) correction factor according to IEC 60904-7 was investigated in detail in order to evaluate the associated uncertainty.

$$SMM = \frac{\int_\lambda E_{\lambda,\text{ref}}(\lambda) \cdot s_{\text{ref}}(\lambda)\, d\lambda}{\int_\lambda E_\lambda(\lambda) \cdot s_{\text{ref}}(\lambda)\, d\lambda} \cdot \frac{\int_\lambda E_\lambda(\lambda) \cdot s_{\text{DUT}}(\lambda)\, d\lambda}{\int_\lambda E_{\lambda,\text{ref}}(\lambda) \cdot s_{\text{DUT}}(\lambda)\, d\lambda}$$

The input quantities for the SMM are the reference spectral irradiance $E_{\lambda,\text{ref}}(\lambda)$, the measured spectral irradiance of the solar simulator $E_\lambda(\lambda)$, the spectral responsivity of the reference solar cell $s_{\text{ref}}(\lambda)$ (mainly crystalline silicon (c-Si)) and the measured spectral responsivity of the device under test $s_{\text{DUT}}(\lambda)$.
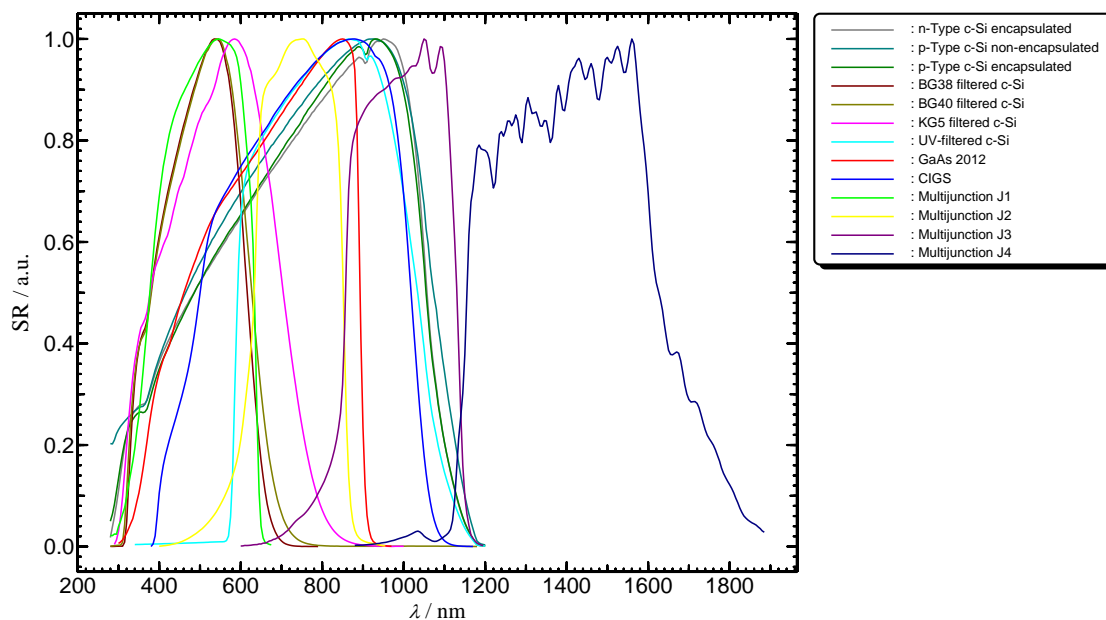

Figure 10: 13 measured and normalized spectral responsivities of different types of PV-technologies provided by PTB. Each SR was folded by slit function with a FWHM of 1 nm, 5 nm, 10 nm, 20 nm and 50 nm to simulate SR measurements of decreasing bandwidth. Additionally the data point interval was reduced respectively.

PTB provided 13 data sets of measured spectral responsivities (see Figure 10) including uncertainties that represent mainly all cases of typical PV technologies (the filtered devices represent different thin film

technologies such as amorphous silicon (a-Si)). For each data set, the spectral responsivity was folded with a triangular slit function with a full width at half maximum (FWHM) of 1 nm, 5 nm, 10 nm, 20 nm and 50 nm to emulate measurement facilities with different bandwidth (*i.e.* from grating monochromator-based systems to filter monochromator systems). The data sets were additionally provided with increased data point interval to emulate different spectral resolution.

PTB, INTA, FhG, ISFH, JRC and SUPSI then performed exemplary SMM calculation on these data sets using their individual numerical tools and procedures. The test case covered an encapsulated *n*-type c-Si solar cell as $s_{\mathrm{ref}}(\lambda)$, a typical Xenon based solar simulator spectral irradiance as $E_\lambda(\lambda)$ and the AM1.5g spectral irradiance as $E_{\lambda,\mathrm{ref}}(\lambda)$.

As a result it was observed that the impact of bandwidth is less than 0.05% for FWHM < 20 nm and the impact of interpolation is less than 0.1% for datapoint intervals < 20nm. The difference between the participating labs and their different mathematical routines was 0.01% - 0.05% for typical cases, in extreme cases up to 0.13%. As a conclusion, these values can be used as estimates to additional measurement uncertainties related to numerical tools dependent on the quality of the available spectral responsivity data.

Further activities dealt with implementing and evaluating the impact of the wavelength-dependent correlations of the input data on the spectral mismatch factor. During a spectral mismatch workshop on December 3rd 2018, PTB, FhG, ISFH, JRC and TÜV Rheinland presented their Monte Carlo-based methods showing that correlations are implemented, but to a different degree for each participant. As a major result of this workshop it was agreed that a comparison on SMM uncertainties is necessary to evaluate the differences between the implemented Monte Carlo tools.

A "worst case" scenario was chosen to evaluate the spectral mismatch correction: Calibration of an a-Si solar cell using a c-Si solar cell as a reference and a class AAA solar simulator (see Figure 11). PTB provided the data set including measurement uncertainties of the input quantities and some additional information of the correlations.
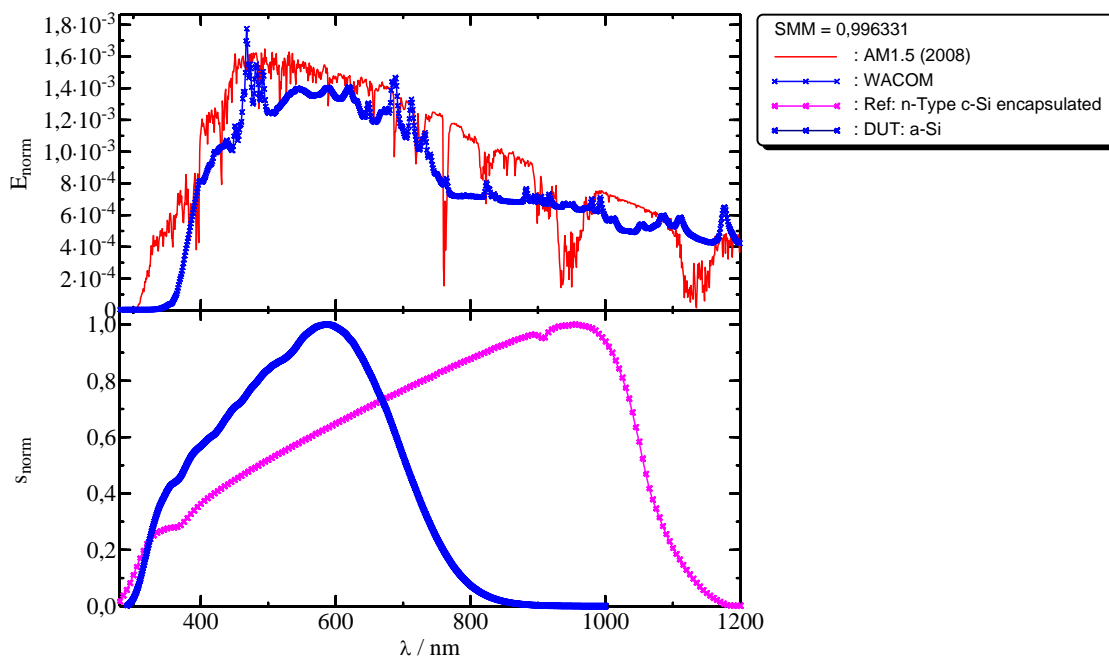

Figure 11: Test case for the comparison of spectral mismatch uncertainties provided by PTB: Calibration of an amorphous silicon solar cell using a crystalline silicon solar cell and a class AAA solar simulator.

The result of this intercomparison is shown Figure 12. The resulting expanded measurement uncertainties for SMM varied from 0.14% up to 0.80%. This demonstrated that the developed methods principally work and deliver similar SMM values. However they lead to strongly different uncertainties.
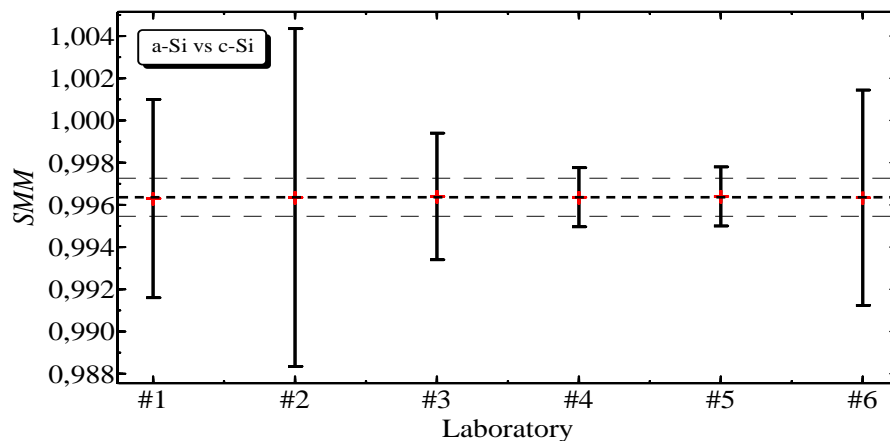
Figure 12: Results of the spectral mismatch correction factor calculation including correlated measurement uncertainties of the laboratories FhG, INTA, PTB, ESTI, ISFH and SUPSI. All laboratories used identical data sets and uncertainties of the input quantities, but their own algorithms for uncertainty propagation. The expanded uncertainty of the SMM varied from 0.14% - 0.80%.

In addition to these intercomparison activities, Aalto has used its newly developed Monte Carlo-based method taking into account possible correlations to analyze three correlation scenarios: (i) no correlation, (ii) combination, and (iii) severe correlation. The corresponding expanded uncertainties were 0.06 %, 0.51 %, and 1.47 %, respectively. These uncertainties provide an estimate of the highest and lowest uncertainties, and the most likely uncertainty. The most likely uncertainty of 0.51%, is located close to the median of the participants of the intercomparison activity, whereas the minimum and maximum values mark the extremes of the comparison.

As a conclusion all partners agreed that there is a need for a well-documented uncertainty analysis for spectral mismatch correction that is available in open access and can act as a general guideline to describe the implementation of measurement uncertainties including correlations in spectral mismatch calculations.

It was agreed that the method should be feasible and simplified so that it becomes applicable. It should base on correlation models that represent true physical origins and it should be possible to evaluate uncertainty contributions in every laboratory.

The approach was chosen as follows:

1. Derive an Ishikawa diagram that includes all possible sources of uncertainties.
2. Find a (simplified) model equation for each source of uncertainty that is quantitatively reasonable and that allows Monte Carlo methods to propagate correlations correctly.
3. Provide all relevant information and guidelines on how to experimentally determine correction factors and uncertainties.
4. Demonstrate the procedure on a typical example

Impact

Since the calibration of spectrometers for measurements of the spectral irradiance caused by solar radiation/solar simulators can be considered to be the most needed guideline for the community, this topic was chosen as the first publication. The paper was written by ISFH and PTB and has been accepted for publication in Metrologia (https://doi.org/10.1088/1681-7575/abafc5). In addition to the publication, the source code for the uncertainty calculation is provided in open access as a template for any interested user (https://isfh.de/dienstleistungen/isfh-caltec/spektralradiometer/).

ISFH, PTB, Aalto, FhG, INTA, ESTI, SUPSI, INTA and LNE worked for this objective that resulted in deliverable D2. For the success of this objective it was required to provide reference measurement data (by PTB), to compare the different approaches of uncertainty measurement calculations (by all) and to write a concluding final paper out of the comparison results (by ISFH, PTB and Aalto with support of the others). As different partners focussed on different methods, this objective could not given such a good overview of the different approaches in use, if it would be done by only one individual partner.

All involved project partners worked on different new realisations for the uncertainty calculation of the spectral mismatch. Those realisations result in uncertainties between 0.05% to 0.8%. PTB provided a set of spectral responsivity curves with low uncertainty as base data for testing the algorithms. An internal workshop "Measurement uncertainties of the spectral mismatch correction" took place to compare the results of the partners which was held one day before the project meeting in December 2018. As a result, from this workshop a comparison between the different realisations took place. This comparison of uncertainties calculations based on the same input data. A general guideline that describes the implementation of measurement uncertainties including correlations in spectral mismatch calculations was developed and published as open access together with the source code of an implementation as open source / open data. The approach derives an Ishikawa diagram that includes all possible sources of uncertainties. It finds a (simplified) model equation for each source of uncertainty that is quantitatively reasonable and that allows Monte Carlo methods to propagate correlations correctly. It provides all relevant information and guidelines on how to experimentally determine correction factors and uncertainties. For illustration it demonstrates the procedure on a typical example. This objective was successfully achieved.

To develop traceable measurement methods for extending energy rating to bifacial solar modules and to modules (bifacial or monofacial) applied to or integrated into buildings. This will include the definition of a harmonised data format for solar device properties, required for PV Energy rating measurement standards (objective 3):

Development of traceable measurement methods for extending energy rating to bifacial solar modules

The aim of this objective is to develop an approach for extending energy rating to include bifacial solar modules. The energy rating of these modules is much more complex than the development of the Standard Test Conditions the first objective as many different scenarios and geometries are imaginable to make use of bifaciality. It is also more complex than the energy rating for standard modules in open rack mounting.

Therefore firstly, relevant conditions different to those for standard modules will be identified. Modelling will then be used to assess the influence on the energy yield. This will then serve as an input for the energy yield assessment of bifacial modules.

In order to assess their performance and quality, mono-facial PV modules are characterized under Standard Test Conditions (STC) as defined by the International Electrotechnical Commission (IEC) [11]. No full international standards currently exist for the characterization of the performance of bifacial modules. In 2019, technical specification (TS) IEC TS 60904-1-2, which provides guidelines for the measurement of current-voltage characteristics of bifacial PV devices, has been published [12]. This TS defines three different approaches including the single-side illumination with a solar simulator (measurements at equivalent irradiance levels) [13], double-sided (simultaneous illumination of both sides using double-source simulators or single-source illumination with a diffuse rear reflector or tilted mirrors) [14] and natural sunlight [15]. IEC TS 60904-1-2 is also a necessary foundation for an extension of the existing energy rating standards to incorporate bifacial devices, since accurate power measurements at defined conditions are essential.

As with mono-facial modules, bifacial modules may be mounted in a number of different configurations. As a further complicating factor, the surrounding albedo also has a significant impact on the performance of the bifacial module. Below are reported some of the most typical current applications of bifacial modules, which may serve as a guide as to which conditions are most representative for being selected for energy rating.
Figure 13 shows bifacial modules mounted on a flat roof on which a high albedo reflective matrix is used to increase power gain and reduce heat load in the building. The modules are ideally equator facing with a fixed tilt. The low inclination angle of 20˚ as used for the mono-facial open rack in the energy rating standard could equally be applicable here. The white reflective roof material has an albedo of typically 60%.

The open rack configuration is also representative of ground-based PV plants, the largest market segment, in which the normally mounted mono-facial modules are replaced with bifacial modules. The modules are ideally equator facing with a fixed tilt. The low inclination angle of 20˚ as used for the mono-facial open rack in the energy rating standard could equally be applicable here. The ground, being dirt or grass has an albedo of typically 20%.

Figure 13: Roof mounted bifacial modules: Fixed tilt 20˚, white roof with albedo = 60%

Figure 14 shows bifacial modules mounted on a single-axis tracker in desert conditions. The tracker increases energy yield of the entire system also for the front surface. Since this mounting configuration is particularly advantageous in desert conditions, the ground albedo considered in this case is that of sand which has an albedo of typically 30%.

Figure 14: Tracked bifacial modules, sand with albedo = 30%

Figure 15 shows bifacial modules mounted vertically in a meadow. This configuration is compatible with dual use, such as agro-PV. This configuration typically employs the modules with an East/West orientation, such that one side face East and the other West. This configuration leads to an increase of output in the mornings and afternoons, and the extra power produced at these times, may be more valuable, even if total energy output may be reduced as compared with an equator facing orientation. The ground albedo considered is that of grass which has an albedo of typically 20%.

The vertical mounting may also be considered representative of the use in acoustic road barriers, where although the orientation is guided by that of the road, the typical albedo of the road surface and surroundings is also around 20%.

Figure 15: Vertical E/W bifacial modules, meadow with albedo = 20%

Table 1 summarises the typical mounting configurations described. The numerical values for orientation, tilt angle and albedo are simplified and selected to be compatible as much as possible with the mounting conditions of the existing standard IEC 61853-4.

Configuration name	Orientation[1]	Fixed/tracked	Tilt angle[2]	Ground albedo[3]
Fixed tilt – roof mounted	Equator	Fixed	20˚	30%
Fixed tilt – ground mounted	Equator	Fixed	20˚	20%
Tracked - desert	Variable	Tracked (single axis)	Variable	50%
Vertical E/W - meadow	E/W	Fixed	90˚	20%
Vertical – road barrier	Variable	Fixed	90˚	20%

([1]) Ideal orientations, equator chosen for simplicity and compatibility with IEC 61853.
([2]) Tilt angles vary in real applications, 20˚ chosen for simplicity and compatibility with IEC 61853.
([3]) Representative values rounded to closest multiple of ten, real values vary.

Table 1: Typical bifacial mounting conditions.

Considering these, already idealised and simplified mounting configurations, it is clear that for the purposes of the creation of an international standard there are vastly too many possible alternatives. In fact, the existing standard IEC 61853-4 for mono-facial modules defines only one mounting condition. Adding too many alternatives for bifacial modules could create confusion and furthermore may not add value if useful differentiation between modules is not obtained in practise. Therefore, we consider the different configurations available and discuss appropriate further simplifications:

Tracked configuration

The use of trackers goes beyond the scope of a standard for modules, so the tracked system can be discounted as an option.

Vertical configuration

The vertical road barrier configuration would be impossible to define precisely since the orientation follows the road and is not fixed, therefore the E/W orientation is the most appropriate choice.

Tilted configuration

It must be taken into consideration in the tilted open rack configuration that the ground based system with albedo of 20% represents a significantly larger market segment, whereas the roof based system with albedo of 60% is a small but growing niche segment. On the other hand, the bifacial gain achievable in the latter case is of potentially more significance. Both options can therefore be analysed further. Maintaining both albedo options would not add significant complexity as the mounting conditions are essentially the same.

To summarise, two basic configurations remain for consideration:

Open rack

An equator facing, fixed tilt 20˚ configuration is compatible with the definition of the existing IEC 61853-4.

Two variants can be studied:

'Roof mounted' with albedo = 60%

'Ground mounted' with albedo = 20%

Both variants require the definition of the rear side irradiance datasets, whereas the front side irradiance dataset is the same as in the existing mono-facial standard.

Vertical E/W

This configuration is not compatible with the definition of the existing IEC 61853-4 and requires the creation of totally new irradiance datasets.

An extension of the IEC 61853 standard series for the energy rating of bifacial modules can be summarised in this way: All 4 parts of IEC 61853 will need to be modified for application to bifacial modules. The proposed extension aims to follows as much as possible the philosophy of the existing standard, while the changes that would be necessary are summarised below.

Part 1: Power matrix with Equivalent Irradiance and Bifaciality Factor. The required maximum irradiance will increase, depending on mounting condition and the albedo chosen. A strong assumption about the uniformity of the rear side irradiance has been made. This may tend to over-estimate the bifacial gain that would be experienced in a real system, and this may be compensated in the tabulated rear side irradiance values by defining lower values.

Part 2: SR and AOI (ar) of the rear side should be measured. The methodology of NMOT measurement most likely will need to be adjusted to the appropriate operating conditions, considering also heating from both sides.

Part 3: Additional calculation steps are required, principally to obtain the equivalent irradiance by summing front and rear side contributions. If the proposed rooftop configuration is to be rated at different elevation above ground than the one considered in the existing standard (2m), this will require an additional step to calculate the wind speed at the defined rooftop height.

Part 4: New hourly data per climatic dataset may be generated using a transposition or other model.

Transposition models (analogous to those used to create the current mono-facial Part 4 datasets) have been implemented to create additional datasets for three of the standard reference climatic profiles. These datasets are used to simulate the full energy rating procedure.

The performance characteristics (c.f. parts 1 and 2 of IEC 61853) of two real c-Si modules have been used to generate two representative bifacial modules, both having a bifaciality of 90%.

The proposed new calculation steps in part 3 of IEC 61853 have been implemented in software and have been used to calculate CSER values for the different bifacial mounting cases for both c-Si modules in order to validate the approach used.

The results show significant differences between the calculated CSER values, between different module types, between different bifacial configurations, and between the mono-facial and bifacial configurations. This

suggests that the proposed modifications could usefully help end-users evaluate and select appropriate bifacial modules with the relevant mounting configuration and climatic profile appropriate to their intended use.

The decision on whether to include either or both of the 20% and 60% albedo cases for the tilted systems, can consider the relative benefits of the differentiation found and the market size of each application. The benefits may need to be set against the anticipated difficulty of measuring the performance matrix up to significantly higher equivalent irradiances than test laboratories are typically able to implement at present.

Development of traceable measurement methods for extending energy rating to building integrated modules

Building integrated photovoltaics (BIPV) are becoming a more and more common installation mode, but complex urban environments and interaction with the building envelope require better consideration of the thermal operating conditions and non-optimal orientation of the modules.

The aim of this objective is to develop an approach for extending energy rating to include modules applied to or integrated into buildings. The energy rating of these modules is much more complex than the development of the Standard Test Conditions in the first objective as many different scenarios and geometries are imaginable for building integrated modules. It is also more complex than the energy rating for standard modules in open rack mounting.

Therefore firstly, relevant conditions different to those for standard modules will be identified. For building integrated modules, representative measurements will be made for conditions not covered by standard energy rating. This will then serve as an input for the energy yield assessment of building integrated modules.

Assumptions for BIPV modules

The translation of real operating conditions into standard reference conditions for Energy Rating purposes has to take into account that the conditions should on one side be specific enough to differentiate between existing BIPV products, but on the other side be as simple as possible to guarantee a high reproducibility of the measurements at a reasonable cost for the customers. This leads to the need to focus on just these conditions, which have a major impact on the 'relative' energy yield. In the case of BIPV these are the thermal operating conditions and the non-optimal orientation of the modules.

The following assumptions are made for the energy rating of BIPV modules:

- • The same modelling procedure as for free-standing (open-rack mounted) modules applies.

- • The module temperatures reached in BIPV modules are significantly higher than for free-standing modules.

- • The best case (optimal ventilation) and worst case (no ventilation at all) conditions are the easiest to implement test conditions and leads to reproducible and comparable test re-sults. Real word lies in-between.

- • The mounting scenarios are limited to the ones showing significant technological differ-ences in energy yield (facade and roof mounting conditions).

- • Coloured mono-facial modules used mainly in the field of building integration do not re-quire any extension of the electrical characterisation procedures except for the application of the adequate BIPV scenario.

BIPV mounting conditions and product diversification

According EN 50583-1:2016 - Photovoltaics in buildings - Part 1 [15] BIPV and BAPV systems can be divided into five mounting categories (see Figure1). The categories are defined as function of the position of the PV system in the building envelope:

- *Category A*: Sloped and roof integrated, not accessible from within the building. PV modules are mounted at an angle between 0° and 75°;

- *Category B*: Sloped and roof integrated, but accessible from within the building. PV modules are mounted at an angle between 0° and 75°;

- *Category C*: Non-sloped (vertically), mounted not accessible from within the building. PV modules are mounted at an angle of between and including both 75° and 90°;

- *Category D*: Non-sloped (vertically), mounted accessible from within the building. PV modules are mounted at an angle of between and including both 75° and 90°;

- *Category E*: Externally integrated, accessible or not accessible from within the building.

Figure 16 shows the mounting categories, whereas Figure 2 gives examples of existing BIPV or BAPV solutions.
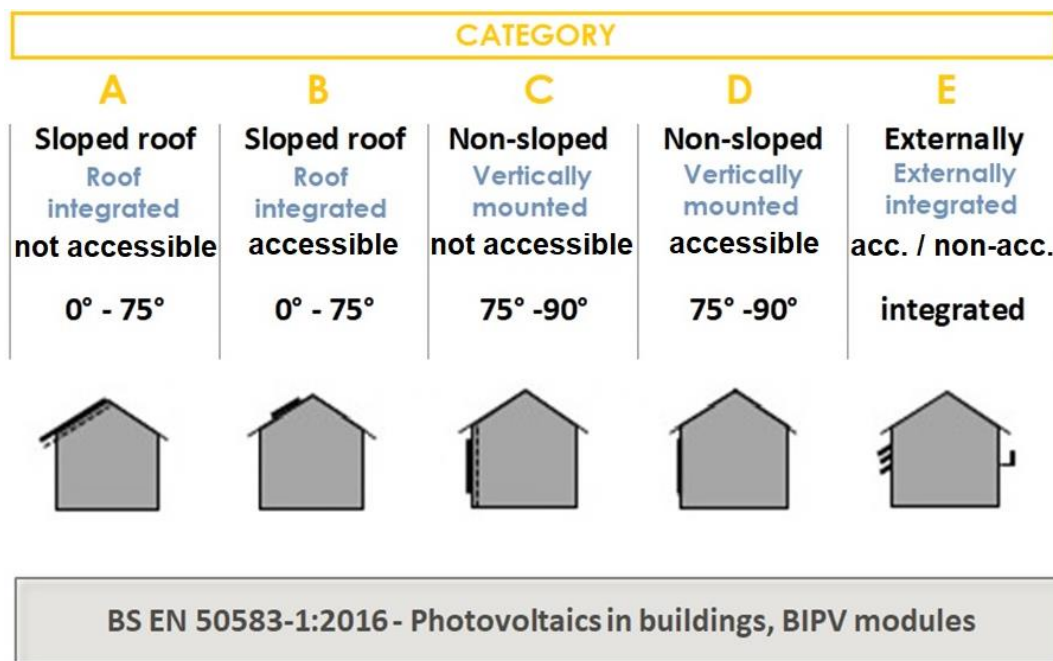

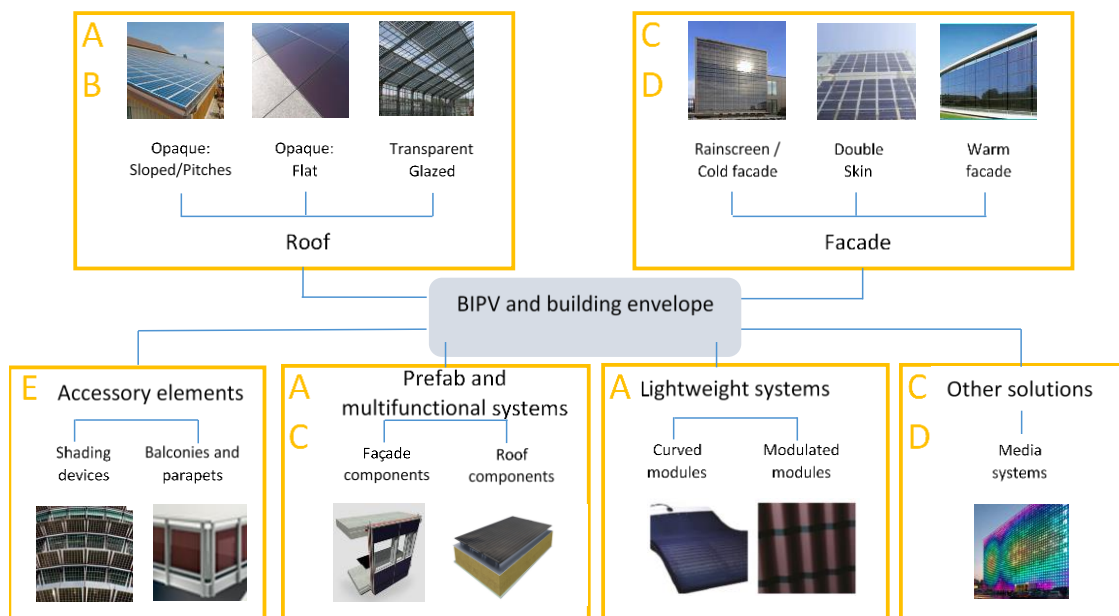**Figure 16:** *Mounting categories A – E (BS EN 50583-1:2016 - Photovoltaics in buildings - Part 1: BIPV modules)*

Figure 17: *BIPV/BAPV possibilities in the building envelope technological systems (source: SUPSI). The scheme also identifies the possible mounting categories (A to E) specified in the new EN 50583-1:2016*

To take into consideration BIPV modules the extension of some parts of the IEC 61853 Standard are proposed. A summary is given in the Box below table 2:

Box 1:   Summary of required extensions to the IEC 61853

Part 1   Power matrix – extension to higher module temperatures.
Part 2   Thermal coefficients (u_0, u_1) to be measured using different mounting conditions and by optimised module temperature measurement procedures.
Part 3   No changes necessary.
Part 4   Reference climatic datasets to be extended to include other tilted surfaces relevant to BIPV, such as façades.

This leads to an extension of the IEC 61853 standard series for the energy rating of BIPV/BAPV modules. The required changes are summarised in the Table 3 below.

IEC 61853	Recommendations	Comments
Part 1: Irradiance and temperature performance measurements and power rating	Extension of the temperature range of the power matrix.	BIPV modules reach higher temperatures than standard modules, the power matrix should be extended to take this into account.
Part 2: Spectral responsivity	none	The current measurement procedures apply also to BIPV/BAPV modules.
Part 2: Incidence angle measurements	none	The current measurement procedures apply also to BIPV/BAPV modules.
Part 2: Module operating temperature measurements	Addition of notes on how to measure module temperature. Addition of 3-6* specific mounting conditions for BIPV/BAPV modules. A differentiation is made between best case, worst case and intermediate ventilation conditions. ** The need to measure u_0 and u_1 for different inclinations is still under investigation.*	The test procedure lacks in details about how to measure the temperature in the case the back of module temperature differs significantly from the cell temperature. There are no indications on how to mount the modules, unless the mounting is described by the module manufacturer. The comparability is so not guaranteed.
Part 3: Energy rating	None* ** except for possible calculation of wind speed at the roof height (h_{roof}) if defined to be different to ground height*	No additional module parameters are required for BIPV/PAPV modules. The equations described in part 3 apply also BIPV/PAPV modules.
Part 4: Standard reference climatic profiles	Addition of a BIPV/BAPV specific scenario for a PV façade. Consideration of a	The standard data set is limited to 20°/equator facing open-rack mounted modules. The data set

	higher wind speed at elevtions above ground level, which would simply define the roof elevation of the system, but would not require any further data.	can be applied for roof mounted modules, but not for façade modules. A façade element is subject to lower irradiances, higher angle of incidences and back-side ventilation. Different product rankings could be obtained when applying this scenario.

JRC, SUPSI, FhG, ISFH, PTB, NPL, TÜV Rheinland, LU and LNE worked for this objective that resulted in deliverables D3 and D4. For the success of this objective it was required to use the experience of the different partners. SUPSI had experience with BIPV and BAPV as it has close connections to the architecture faculty that no other partner could provide. FhG and ISFH could provide long standing experience with the modelling of bifacial testing condition. TÜV Rheinland, FhG, JRC and LU had first experience in the measurement of bifacial PV devices. This knowhow was combined with the metrological and radiometrical knowledge of the NMIs PTB, NPL and LNE. Thus, also for this objective it was important to combine the knowhow of the different partners and it could not have been successful, if it would be done by only one individual partner.

An extension of the IEC 61853 standard series for the energy rating of bifacial modules has been described. All 4 parts of IEC 61853 will need to be modified for application to bifacial modules. The proposed extension aims to follows as much as possible the philosophy of the existing standard, while the changes that would be necessary are summarised below.

The results show significant differences between the calculated CSER values, between different module types, between different bifacial configurations, and between the mono-facial and bifacial configurations. This suggests that the proposed modifications could usefully help end-users evaluate and select appropriate bifacial modules with the relevant mounting configuration and climatic profile appropriate to their intended use.

An extension of the IEC 61853 standard series for the energy rating of BIPV/BAPV modules has been described, too. It requires changes in different parts of the energy rating standards series IEC 61853. Part 1 must be extended as BIPV modules reach higher temperatures than standard modules. In Part 2 the mounting conditions for BIPV modules must be added to enable comparability between different manufacturer. In part 4 of the IEC 61853 series additional BIPV/BAPV specific scenario for a PV façade would be useful, especially the consideration of a higher wind speed at elevations above ground level, which would simply define the roof elevation of the system, but would not require any further data. The standard data set is limited to 20° equator facing open-rack mounted modules. The data set can be applied for roof mounted modules, but not for façade modules. A façade element is subject to lower irradiances, higher angle of incidences and back-side ventilation.

This objective was successfully achieved.

To enable instantaneous measurement of the spectral radiance of the complete sky for improved determination of real outdoor measurement conditions and the irradiance spectral-angular distribution by hyperspectral imaging (objective 4):

Enabling instantaneous measurement of the spectral radiance of the complete sky

The aim of this objective is to measure the spatial distribution of the spectral sky radiance under different weather conditions and various cloud cover situations (clear sky, partly cloudy and cloudy) during a two months' measurement campaign at LUH using two different outdoor measurement systems – (a) LUH's Advanced Multidirectional Spectroradiometer (AMUDIS) and b) PTB's Skyscanner.

The AMUDIS is a worldwide unique multidirectional spectralradiometer developed at the LUH capable of measuring radiance in the wavelength range from 250 nm – 1700 nm in more than 100 different directions simultaneously with a high spectral and temporal resolution. PTB's Skyscanner was developed within the EMRP ENG55 PhotoClass project and is now operational. The measurements and the comparison of the two distinct systems will lead to a better understanding of the measurements and the various uncertainties sources, enabling a reduction of the overall measurement uncertainty.

This paragraph summarizes the intercomparison of spectral sky radiance measurements perfomed in July and August 2019 at the rooftop platform of IMUK in Hannover. Two measurement setups are involved in this intercomparison: LUH's AMUDIS and PTB's Skyscanner system. A three weeks' measurement campaign has been performed to obtain spectral sky radiance datasets under various cloud cover situations (clear sky, partly cloudy, diffuse (hazy), and overcast). A comparison of the data obtained by the partners during the campaign is presented.

Figure 18: Photograph of the scanning PTB's Skyscanner on the right-hand side and the LUH's AMUDIS on the left-hand side during the intercomparison at the rooftop platform of IMUK institute of LUH in Hannover.

The PTB Skyscanner system was developed within the ENG55 PhotoClass project. To perform intercomparing measurements with LUH's AMUDIS an entrance optics has been enhanced to obtain shorter integration times

by larger signals (factor of six), and thus a faster scanning procedure. The enhanced entrance optics provides a field of view of 7.5°, which is comparable to the average field of view (8°) of the AMUDIS VIS channels.

Prior to the outdoor measurements PTB's Skyscanner system has been calibrated against a standard lamp and a reflectance standard. The wavelength traceability is ensured by spectral lamps using atomic emission lines (pencil lamps).
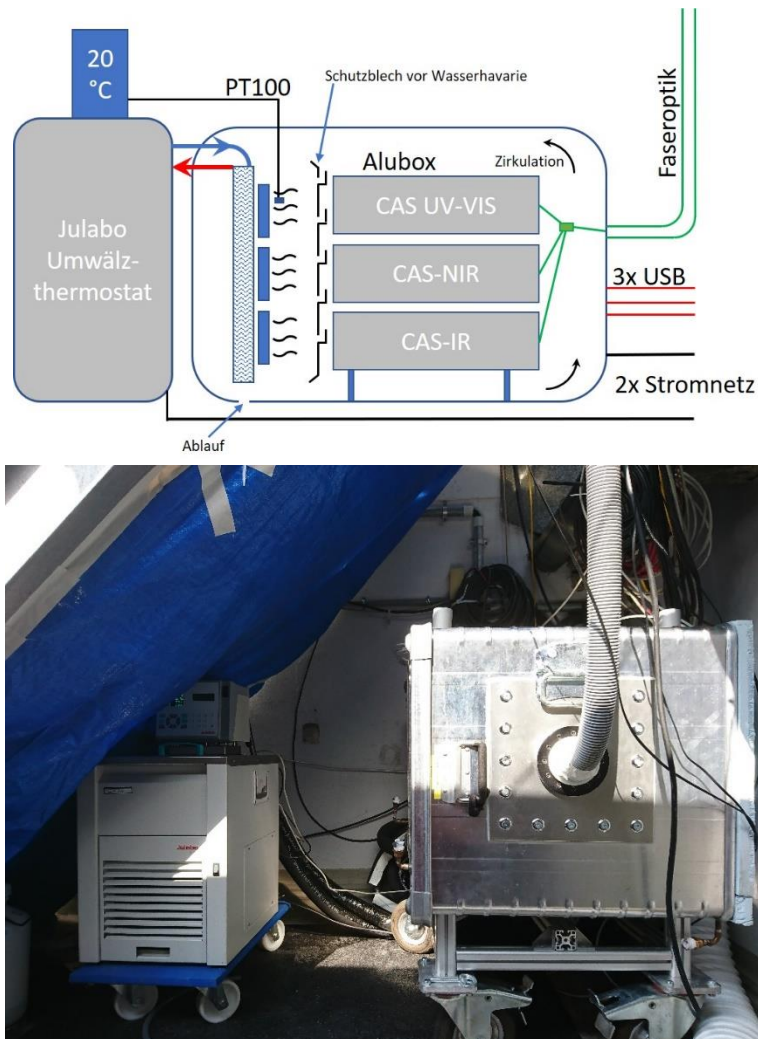

Figure 19: (Top) Cooling concept of PTB's Spectroradiometers in a thermobox; (Bottom) Photograph of the thermobox on LUH's roof.

To ensure a stable operation under enormous heat load, temperature fluctuations, and to provide protection of the instruments against various weather conditions, a thermobox has been designed and tested prior the measurement campaign. The thermobox consists of a laboratory chiller and a weatherproof aluminum box, that includes a cooling fans and heat exchanger for cooling and heating water (see Figure). A temperature logger is used during the campaign monitor possible fluctuations in temperature and humidity. A temperature stability of better than ± 1.5 K was achieved with this improvised solution.

The measurements were carried out during daytime mainly from 09:00 a.m. to 05:00 p.m. To ensure simultaneous measurements the systems clocks were synchronized with an accuracy well below ± 1 second.

summarizes the different weather conditions (except rainfall) occurred during the measurements taken at the measurement campaign. The assignment of sequence numbers shall facilitate the data evaluation procedure for the comparison.

Condition	occurrence	Sequence numbers
Partly cloudy	24	#002, #003, #004, #005, #006, #007, #008, #012, #013, #014, #015, #026, #027, #028, #029, #032, #033, #034, #035, #041, #042, #043, #044, #045
Cloudy	7	#009, #010, #021, #023, #024, #025, #047
Less cloudy	2	#011, #012
Broken clouds	4	#013, #023, #024, #025
Clear sky	5	#030, #031, #032, #048, #049
Diffuse conditions (haze)	3	#037, #038, #039
Overcast	7	#016, #017, #018, #019, #020, #021, #047
Dark overcast	1	#046

Table 4: Measured conditions with the PTB Skyscanner system

Data acquisition and Evaluation procedure of PTB datasets

PTB's Skyscanner system needs approx. 20 seconds per position. At each single position an auto ranging routine is performed for each of the two spectroradiometer channels (VIS and NIR) used in this intercomparison. This ensures enough signal and prevents the device from being oversaturated. Afterwards, the spectrum is measured using the optimum integration time, and subsequently a dark current measurement using the same integration time. For the less sensitive channel (NIR) a maximum integration time of 5000 ms is chosen, to limit the time consumed at each position. Each measurement provides a timestamp and the corresponding position number (see Table). The orientations of positions number 0, 1, 75, 148 highlighted in yellow, are measured in addition to the orientations covered by AMUDIS.

The raw data captured with PTB's spectroradiometers is processed as follows:
Our data evaluation procedure converts the absolute values (radiance) from the measured raw data (counts per millisecond). The dark current (counts per millisecond) is subtracted for each single measurement using the corresponding dark measurement achieved with a mechanical shutter. The evaluation procedure includes beside a wavelength correction also a correction for internal spectral straylight for the VIS-channel. The straylight correction was determined prior the campaign using a tunable laser system. The two spectra obtained by using two separate channels overlap each other. Both spectra are merged at a wavelength of 900 nm.
The corrected spectra are finally exported into *.txt ASCII files. Each spectrum file includes a header with information about time, position and the radiance integrated between 300 nm and 1600 nm.
Figure20 shows a set of spectral radiances $L\lambda$ measured under clear sky on the 8th August of 2019.

Position (PTB)	azimuth/ °	zenith / °	Position (PTB)	azimuth/ °	zenith/ °	Position (PTB)	azimuth/ °	zenith/ °
0	direct	sun	50	108	52.5	100	231.43	73.5
1	0	15	51	112.5	42	101	234	52.5
2	0	0	52	112.5	84	102	236.25	84
3	0	10.5	53	115.71	73.5	103	240	31.5
4	0	21	54	120	31.5	104	240	63
5	0	31.5	55	120	63	105	244.29	73.5
6	0	42	56	123.75	84	106	247.5	42
7	0	52.5	57	126	52.5	107	247.5	84
8	0	63	58	128.57	73.5	108	252	52.5
9	0	73.5	59	135	21	109	255	63
10	0	84	60	135	42	110	257.14	73.5
11	11.25	84	61	135	63	111	258.75	84
12	12.86	73.5	62	135	84	112	270	10.5
13	15	63	63	141.43	73.5	113	270	21
14	18	52.5	64	144	52.5	114	270	31.5
15	22.5	42	65	146.25	84	115	270	42
16	22.5	84	66	150	31.5	116	270	52.5
17	25.71	73.5	67	150	63	117	270	63
18	30	31.5	68	154.29	73.5	118	270	73.5
19	30	63	69	157.5	42	119	270	84
20	33.75	84	70	157.5	84	120	281.25	84
21	36	52.5	71	162	52.5	121	282.86	73.5
22	38.57	73.5	72	165	63	122	285	63
23	45	21	73	167.14	73.5	123	288	52.5
24	45	42	74	168.75	84	124	292.5	42
25	45	63	75	180	0	125	292.5	84
26	45	84	76	180	10.5	126	295.71	73.5
27	51.43	73.5	77	180	21	127	300	31.5
28	54	52.5	78	180	31.5	128	300	63
29	56.25	84	79	180	42	129	303.75	84
30	60	31.5	80	180	52.5	130	306	52.5
31	60	63	81	180	63	131	308.57	73.5
32	64.29	73.5	82	180	73.5	132	315	21
33	67.5	42	83	180	84	133	315	42
34	67.5	84	84	191.25	84	134	315	63
35	72	52.5	85	192.86	73.5	135	315	84
36	75	63	86	195	63	136	321.43	73.5
37	77.14	73.5	87	198	52.5	137	324	52.5
38	78.75	84	88	202.5	42	138	326.25	84
39	90	10.5	89	202.5	84	139	330	31.5
40	90	21	90	205.71	73.5	140	330	63
41	90	31.5	91	210	31.5	141	334.29	73.5
42	90	42	92	210	63	142	337.5	42
43	90	52.5	93	213.75	84	143	337.5	84
44	90	63	94	216	52.5	144	342	52.5
45	90	73.5	95	218.57	73.5	145	345	63
46	90	84	96	225	21	146	347.14	73.5
47	101.25	84	97	225	42	146	347.14	73.5
48	102.86	73.5	98	225	63	147	348.75	84
49	105	63	99	225	84	148	direct	sun

Table 5: Scanning pattern of the PTB Skyscanner system. (Azimuth orientation: 0° -> North; 90° -> East; 180° -> South; 270° -> West)
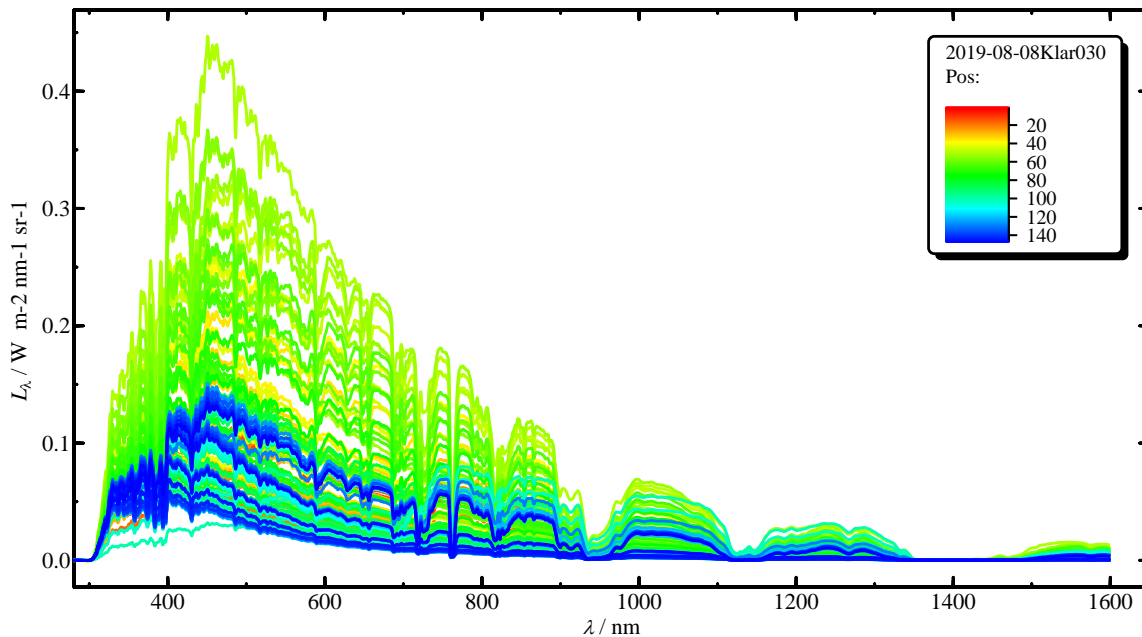
Figure20: Spectral sky radiance under clear sky conditions, measured from 09.28 a.m. to 10:21 a.m. on the 8th August 2019. (Position 0, 50 and 148, were the direct sunlight was measured are not shown)

After returning the measurement system to PTB, a second calibration measurement of the spectral radiance was performed to validate the calibration and to test the stability of the system after a period of more than three weeks. For both calibrations (prior and afterwards), a 150W tungsten halogen lamp and a BaSO4 reflectance standard were used.
To obtain the instruments responsivities 250 consecutive measurements were averaged for the VIS-channel and 100 for the NIR-channel.

Figure shows a comparison of both calibration values CV and for each channel separately. The black curves indicate the differences respectively. The difference for the VIS-Channel is below 1% for wavelengths larger than 360 nm. Within the wavelength region between 300 nm and 360 nm the maximum difference is below 5 %.

However, the NIR-channels differences in the two CV's are lower than 2 % over the entire wavelength range. Obviously, the CV of the VIS-Channel which was measured after the campaign is larger than measured prior the campaign, and the differences of CV's of the NIR-Channel are the other way around.

The evaluation of the measurements with the AMUDIS unfortunately failed within the extended project time due to the complexity of the measurement and evaluation process. Thus, at the current stage of development the AMUDIS cannot be recommended for the spectrally and angularly resolved measurement of the irradiance or the spectral radiance of the sky. Despite the limitations regarding the simultaneity of the measurements, only PTB's scanning system (Skyscanner) can be recommended at this time. Both institutes will further develop their measuring systems to reduce the existing limitations.
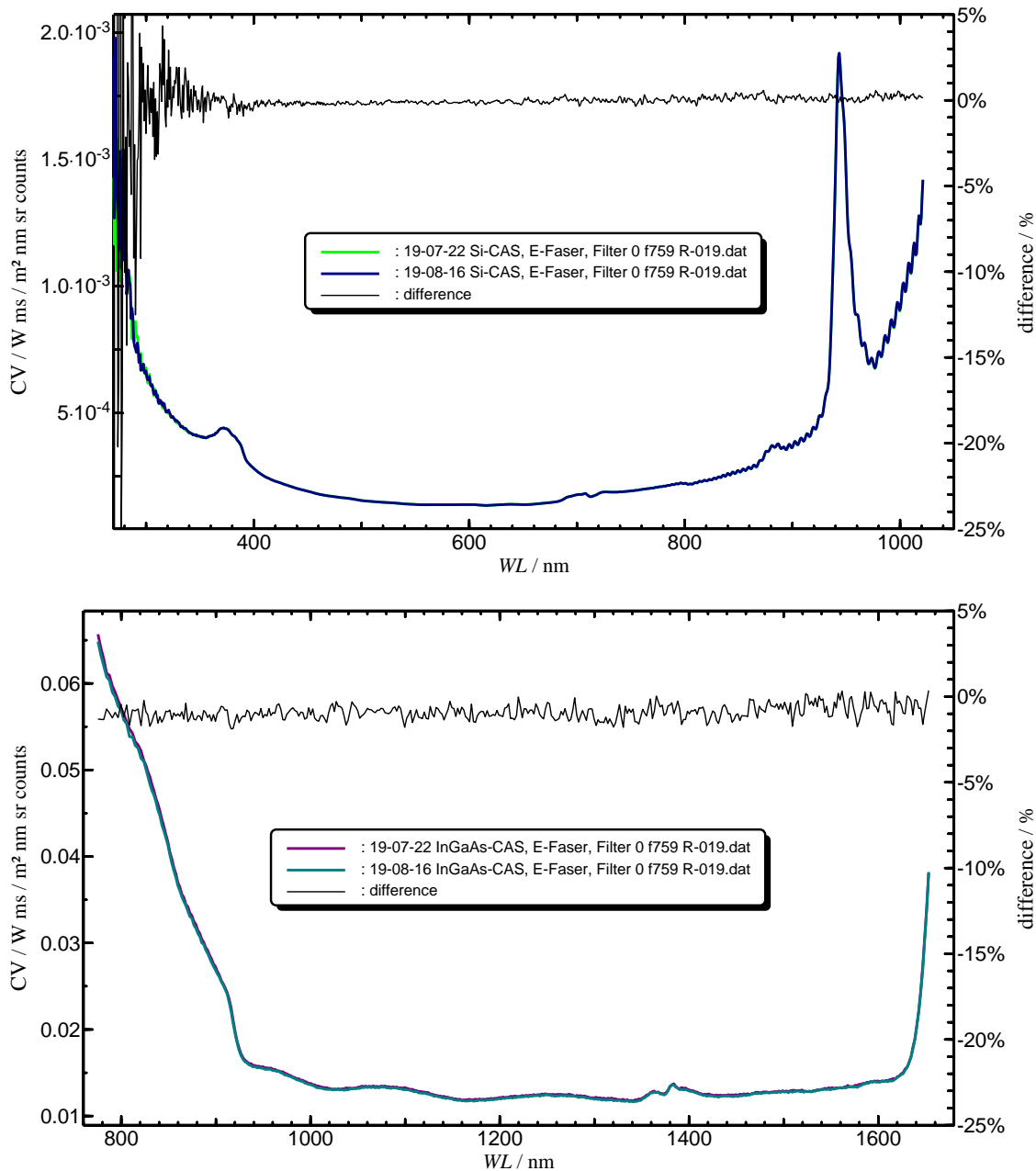
Figure 21: (Top) Comparison of the responsivity of the VIS-Channel. The green line indicates the calibration performed on the 22th of July 2019, prior the campaign, and the dark blue line indicates the calibration performed after the campaign on the 16th of August 2019. (Bottom) Comparison of the responsivity of the NIR-Channel. The purple line indicates the calibration performed on the 22th of July 2019, prior the campaign, and the cyan line indicates the calibration performed after the campaign on the 16th of August 2019. Black lines indicate the percentage difference of the calibration taken afterwards relative to the calibration prior the campaign for both, top and bottom figures.

PTB and LUH worked for this objective that resulted in deliverable D6. For the success of this objective it was necessary to compare the existing measurement system with the world-wide unique hyperspectral sky scanning system that was invented by Prof. Seckmeyer of LUH. This objective could not have been started, if it would be done by only one individual partner.

The intercomparison of spectral sky radiance measurements has been completed in Summer 2019. The comparison took place at the roof of LUH. Two different measurement facilities were compared. One portable sky-scanning facility of PTB scanned the sky direction by direction within 30 minutes and measured at all

direction the spectral radiance. The AMUDIS facility of LUH measured the spectral sky radiance of nearly 150 directions simultaneously. The evaluation of the scanning facility has been finished. The evaluation of the measurements with the AMUDIS unfortunately failed within the extended project time due to the complexity of the measurement and evaluation process. Thus, at the current stage of development the AMUDIS cannot be recommended for the spectrally and angularly resolved measurement of the irradiance or the spectral radiance of the sky. Despite the limitations regarding the simultaneity of the measurements, only PTB's scanning system can be recommended at this time.

This objective was partly successfully achieved. The direct comparison of the two methods were not successful, nevertheless a recommendation concerning the methods can be given.

To develop more accurate measurement methods for traditional and emerging solar modules, including the spectral responsivity of the complete module, fast linearity measurements for modules, angular dependency of modules, with an uncertainty of <1 % for the angular dependency impact, <3 °C for the nominal operating module temperature (NOMT), <1 % for the impact of spectral responsivity and <1 % for the impact of non-linearity:

Development of more accurate measurement methods for traditional and emerging solar modules

The aim of this objective is to improve existing measurement methods for different types of traditional and emerging photovoltaic modules.

Setup of an LED-based solar simulator with a 5-axis PV module holder

The aim of this task is to develop new characterisation methods for PV modules that go beyond the current limitations in PV metrology. The significant challenges for PV module characterisation and calibration are to combine the lowest uncertainty of 1.2 % with fast measurements for PV module-sized devices.

For this an LED-based solar simulator has been set up at PTB in 2018 (Figure 20). The LED light source is a prototype developed by the company Wavelabs and has only be set up at three different sites up to now. By thorough characterization and feedback loops with the developers, the PTB system is the most advanced system regarding its stability and non-uniformity up to now. In addition, an electrically driven five-axis PV module holder has been set up. For both instruments suitable LabVIEW control software for system automation purposes has been written, this enables us to highly automate the measurement process.

The system has been subsequently characterized for homogeneity (Figure 23), stability (Figure 24) and spectral quality (Figure 25). Especially high-resolution non-uniformity measurements could be performed well with the five-axis module holder system enabled us to calculate the specific non-uniformity of any given device under test.
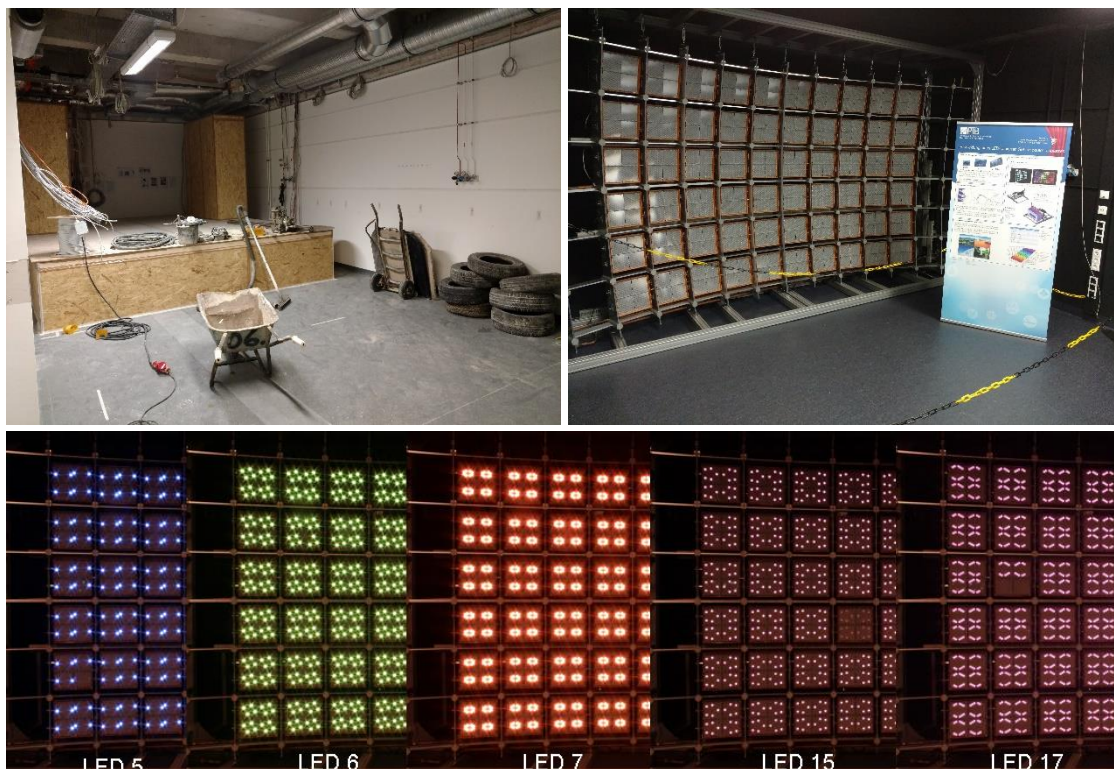
Figure 22: Upper left: PV module laboratory during construction in 2017. Upper right: LED-based solar simulator in completed laboratory in 2018. Lower plot: LED solar simulator with different LEDs turned on.
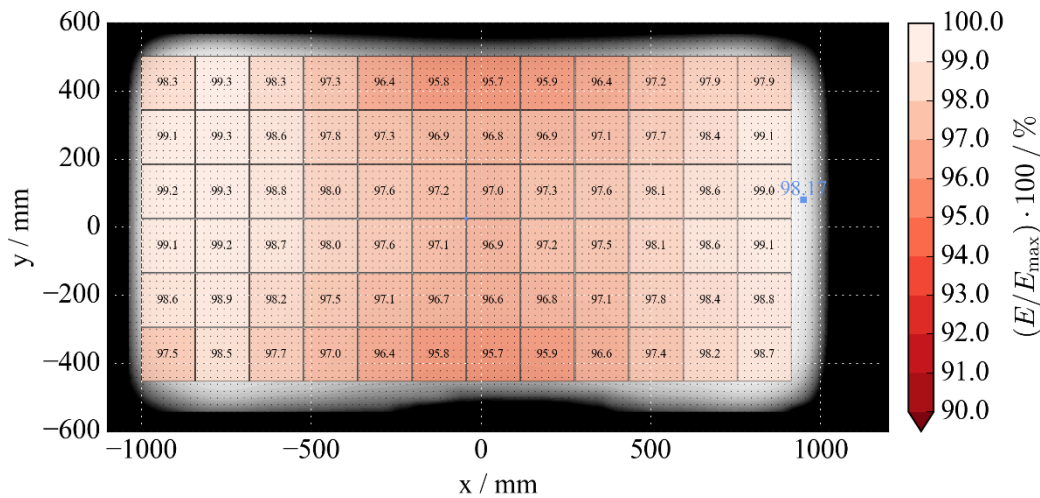
Figure 23: 72-cell module simulation based on a high-resolution scan of the light field. The blue marker is the position of the WPVS reference cell used for calibration of the system. A correction factor for the specific module and reference position can be derived for IV curve corrections.
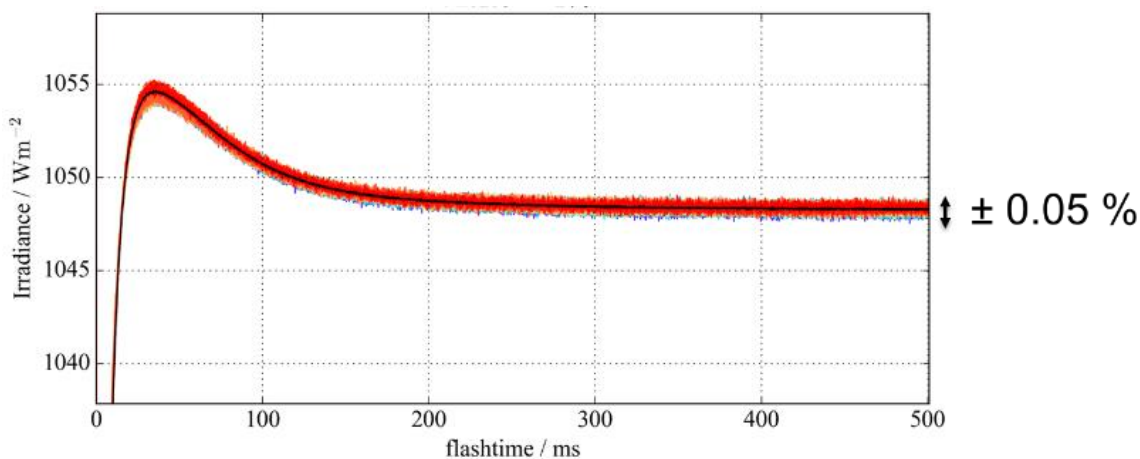

Figure 24: Repeatability of 50 consecutive LED flashes shows an expanded standard deviation of +-0.5 %. In-flash drift is acceptable low after 150 ms, total flash length was 500 ms.
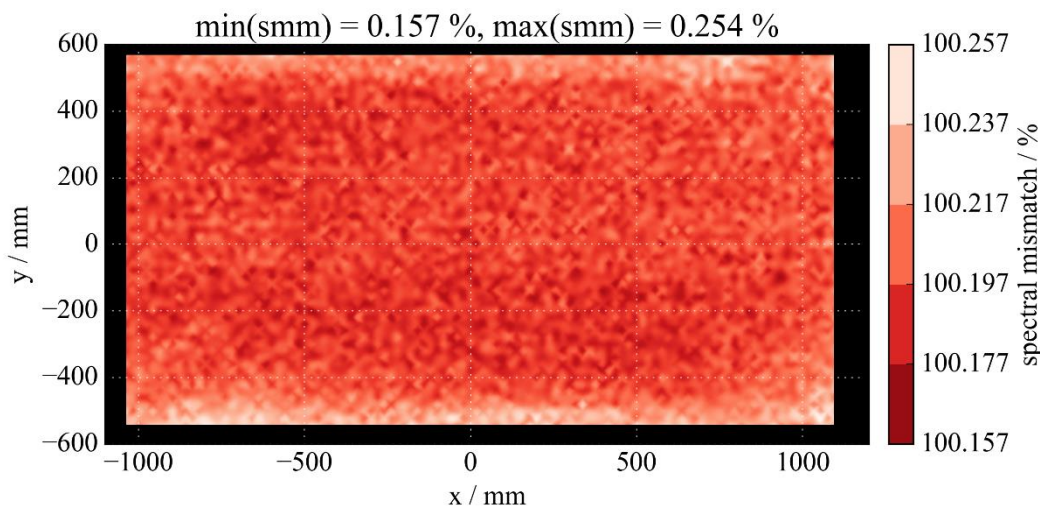

Figure 25: Spatial deviation of the spectral mismatch between WPVS refewrence cell and a typical Si-based module. The SMM is rather low and the variation of the SMM is less than 0.1 % over the test area and mostly apparent only at the edges.

DLP light source upgrade

At NPL as a first option, a 256-LED single-cell prototype of a new modular light source has been developed, which has the size of a conventional wafer size silicon cell (156 mm x 156 mm). The aim was to develop a prototype which would consist of 6 of these light sources, on order to be able to measure a mini module. The prototype worked for individual cells but the lead time to manufacture all of the system with the multiple light sources fell outside the project's timeline.
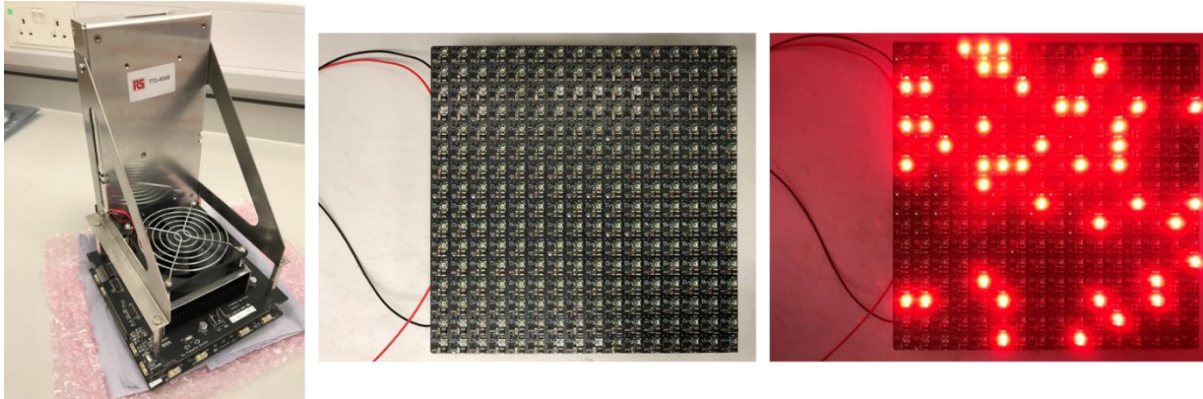
Figure26: The 256 LED digital light source delevoped at NPL. Each LED pixel can be individually configured.

An alternative route was eventually followed to implement the activities, this was the development of a DLP light source, upgraded with new projection optics and coupled with a high-power LED light source of 200 W. This can be used to provide spatially modulated light on individual cells, achieving irradiance levels of more than one sun on wafer sized silicon cells. Across a 6-cell mini-module irradiance levels of around 50 W/m2 can be achieved since the beam is significantly expanded. For this reason, the DLP light source has limited power for measuring linearity over large areas. The main limitation that is bound to any DLP system is that the digital micromirror device (DMD) that the DLP system is based upon has an optical power limit of 25 W. This is the maximum power that can eventually come out of the DMD. A second large-area light LED light source can be used to provide modulated output over larger areas. The DLP light source has been tested and is ideal for solar cells up to 200 mm by 200 mm area. The light source was used to realize the other relevant activities
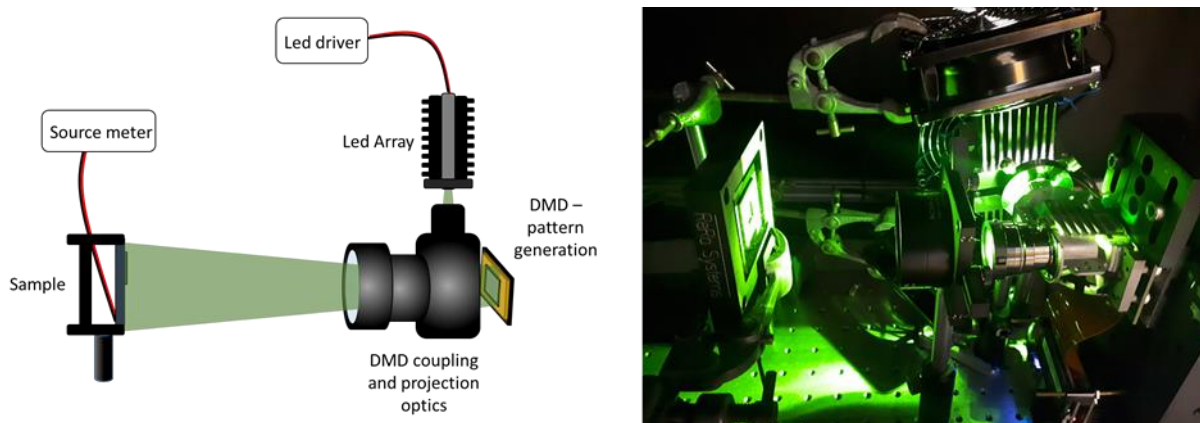

Figure27: DLP setup with the new 200 W LED light source. The setup is capable of illuminating cells with specific patterns, replacing a mesh filter.

Setup for spatial dependence of power generation from PV modules

NPL has developed an algorithm for extraction of IV curve parameters from individual series-connected cells in a module. In order to extract I-V curves of individual cells of a fully encapsulated PV module, a number of I-V curves of the module has to be acquired. For a specific cell of the assumed module, a series of predefined shading levels are applied on the cell while the rest of the module is fully illuminated, with I-V curves of the module acquired for each shading level. This procedure is repeated for all cells, leading to the acquisition of a set of I-V curves of the module. Assuming a specific modelling representation of the PV module and given an arbitrary number of I-V curves with different shading levels that can be acquired for each cell, an optimization problem is defined. The solution of the optimization problem eventually provides the estimates of the I-V curve parameters for each cell.
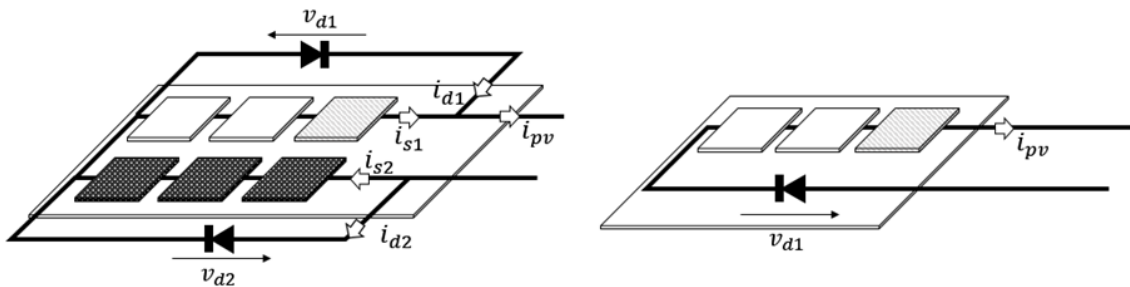
Figure28: Approximation of the bypass diode connections in presence of strong shading, applied by a DLP system for I-V extraction of individual cells of a 6-cell mini module. The complete circuit is shown on the left, the approximation used in this work for calculations is shown on the right.

The approach was validated in a simulated environment through statistical analysis, with the cell parameters based on real silicon PV devices. The computational complexity of the approach was also investigated and validation examples with different configurations of PV modules, including bypass diodes were studied. The approach was validated on several tests to assess noise robustness, flexibility in terms of cells non-uniformities and scalability towards larger systems, resulting in a lean and accurate procedure for I-V curves extraction. A set of results for a module with twelve cells including defects and three bypass diodes is presented in Figure29, where the efficiency of the method is demonstrated.
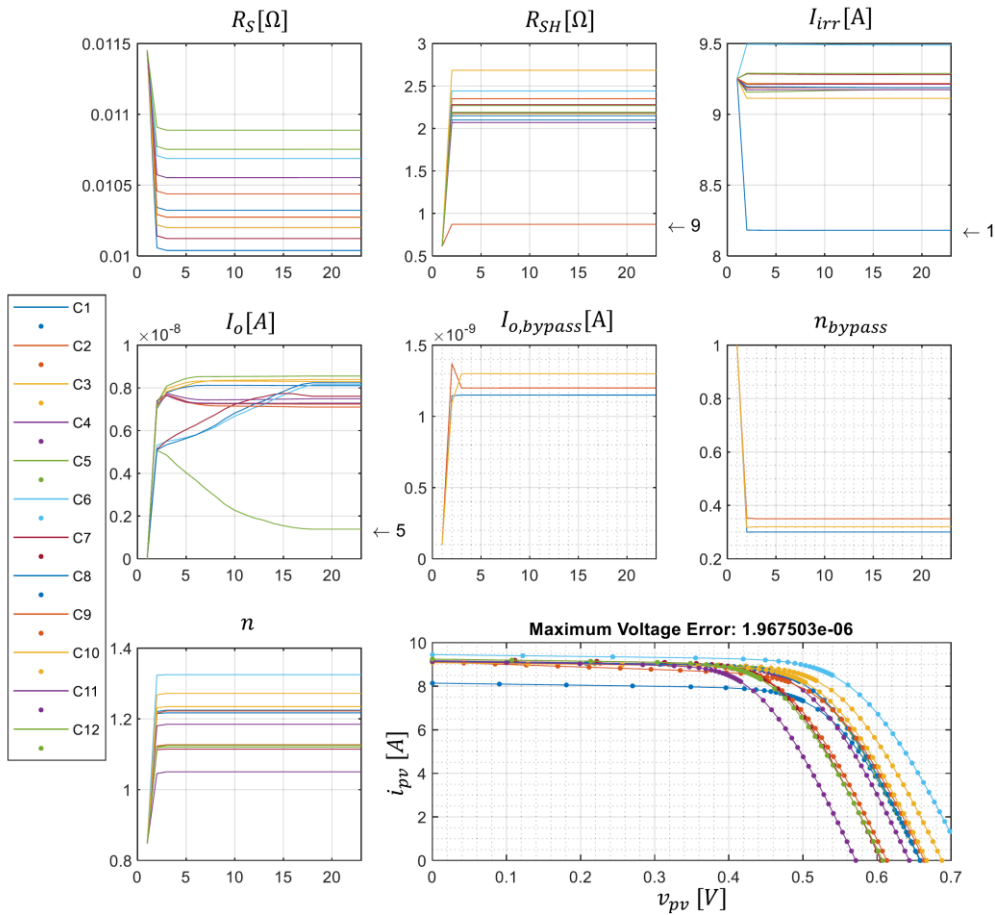
Figure29: Parameters extraction progress monitor. The large plot shows the result of the extraction procedure, superimposing the real cells I-V curves (dots) from the validation dataset, against the curves found by the extractor (solid lines), with added plots for the bypass diodes parameters. The arrows relative to the parameters of non-uniform cells (i.e. cells 1, 5 and 9) are shown next to the curves. The steady value reached at iteration 24 corresponds to the original parameters of the cells.

This methodology requires that a number of different well-defined irradiance levels can be used for every cell. The DLP projection system developed in A3.1.3 is used to provide the different irradiance levels. Tests with the DLP system at NPL and at LU demonstrated that the irradiance is rather low for the algorithm to be implemented consistently. Additional accurate EL imaging data are required in order to define all parameters required as inputs for the algorithm. A much higher power light source would be required to implement the method accurately and apply the algorithm for a PV module. The measurement acquisition for the tests that the algorithm requires lasts only 15 s. The algorithm, methodologies and results were published in Blakesley et al. 2020.

Figure 30: Pictures of the measurement procedure for I-V curve extraction, the DLP system projects a series of patters on the PV module to be measured. On the left, the series of patters are on the top middle cell of the mini module, on the right, the series of patterns are on the bottom right cell, the procedure described above is followed.

Optical and electrical characterisation of emerging PV modules (BIPV modules)

More and more coloured modules with special glass, treated front covers, printed surfaces, etc. are entering the BIPV sector, often driven by the need to satisfy a growing aesthetical demand from architects. However the "price" of these aesthetics can be a lower final power output and yield. Whilst power loss from PV modules is easily measurable under standard test conditions, their performance under real operating conditions and knowledge of how the modules should be characterised to accurately reflect the real operating environment is not fully understood.

The aim of this sub-objective is to identify the main requirements needed to describe and measure the performance of new special BIPV modules that have recently or are currently entering the market.

An internal report was prepared by SUPSI giving an overview on existing BIPV solutions and technological trends that will have the chance to emerge within the next 5 years. The customization of BIPV products varies from the scale of the module (e.g. choice of solar cell technology, the shape and dimension of cells or module, the type/colour of materials, the electrical contacts or modifications in electrical design to change the appearance, the transparency, structured front glass, back side materials etc.) up to the complete building system. The impact the customization of PV modules has on energy production is discussed in a second report. Figure31 shows a picture of a mock-up installed in Lugano demonstrating variants and possibilities in terms of architectural and technological design.

SUPSI assessed the measuring procedures for the optical and electrical characterisation of special and customised BIPV modules for the purpose of energy rating. Characterization of some coloured BIPV modules were performed. The results were presented within the consortium and shared for various modelling activities.

Figure31: Façade mock-up developed within Construct PV FP7 Project (http://www.constructpv.eu) and mounted in Lugano. The mock-up demonstrates variants and possibilities in terms of architectural and technological design/manufacturing of BIPV systems for the building skin (Source: SUPSI).

Improvement of spectral responsivity measurements for solar modules

The (differential) spectral response (DSR/SR) technique based upon conventional light sources such as halogen lamps and Xenon arc lamps is currently applied for the calibration of reference solar cells with the lowest uncertainties. However, due to low monochromatic irradiance, this technique is restricted to small solar cell sizes and is not applicable at the module level.

To overcome this limitation at the PTB LED-based solar simulator a DSR measurement technique for PV modules has been developed and tested on different silicon based and thin film PV modules. The method has been published in (Sträter et al. 2019). Up to now, the method has been applied to various module techniques, including mSi, pSi, CdTe, CIGS and bifacial modules. Figure32 shows the results of our internal comparison with a well-known WPVS reference cell calibrated at the DSR cell facility at PTB.
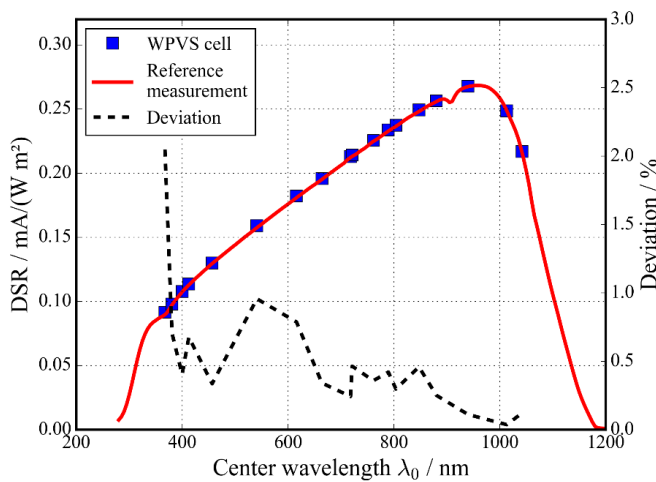
Figure32: Results of the spectral responsivity measurement conducted solely with the LED solar simulator. The results have been compared with an WPVS reference measurement conducted at the DSR cell facility at PTB.

At TUBITAK UME, the spectral responsivities of monocrystalline, polycrystalline, CIGS thin film and bifacial PV modules were measured according to the IEC 61853-2 and IEC 60904-8 standards. To implement these methods described in this standard a xenon light-based pulse type solar simulator system and a set of 15 different band pass filters having 50 nm band width from 400 nm to 1100 nm wavelength interval were used. A suitable fitting algorithm was also applied in order to derive the SR curves based on the 15 measurement points (see Figure 18).
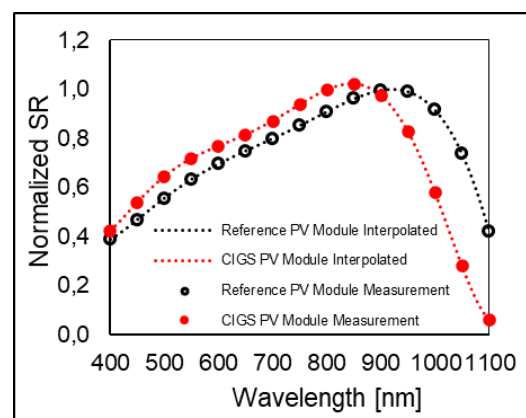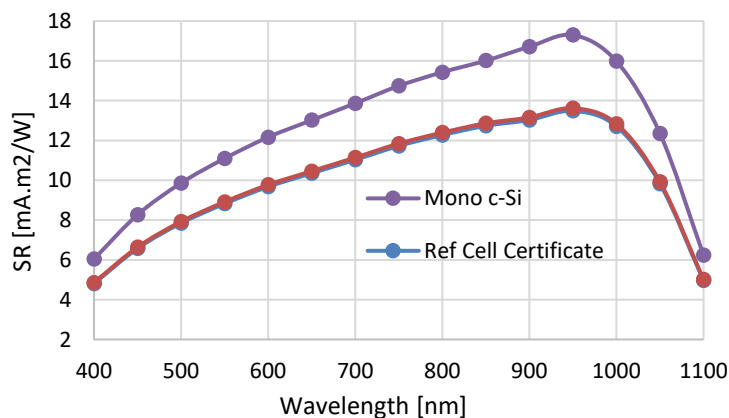

Figure 18: Example for SR measurements conducted at TUBITAK UME.

In order to compare the determination of spectral responsivity between an LED-based setup at PTB and a Xenon-based solar simulator setup at TUBITAK, a bidirectional comparison with a poly-Si module has been

carried out. While differences between 400 and 700 nm are low, the SR measured at PTB shows an overestimation at several measurement points between 700 and 900 nm. The reason for these deviations is not yet found, we assume a connection to the varying bandwidth of the LED channels of the LED solar simulator. However, if a spectral mismatch correction is conducted with both SR curves, the difference of the correction factors is 0.06 % for a typical combination of poly-Si module, mono-Si reference cell and the PTB solar simulator system.
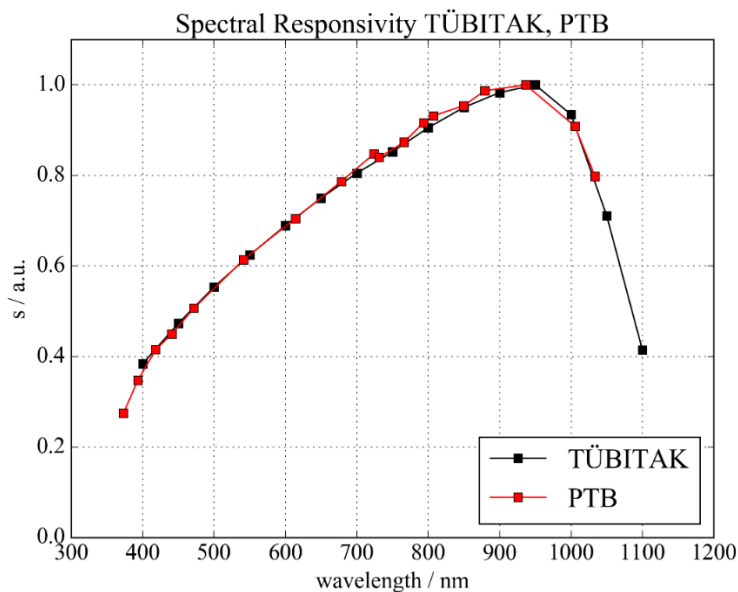
Figure 19: Spectral responsivity comparison between PTB and TUBITAK for a poly-Si module.

SUPSI focused on the characterization of colored modules and its spectral response curves. 8 different modules were measured, results were shared within the consortium (e.g. Figure).
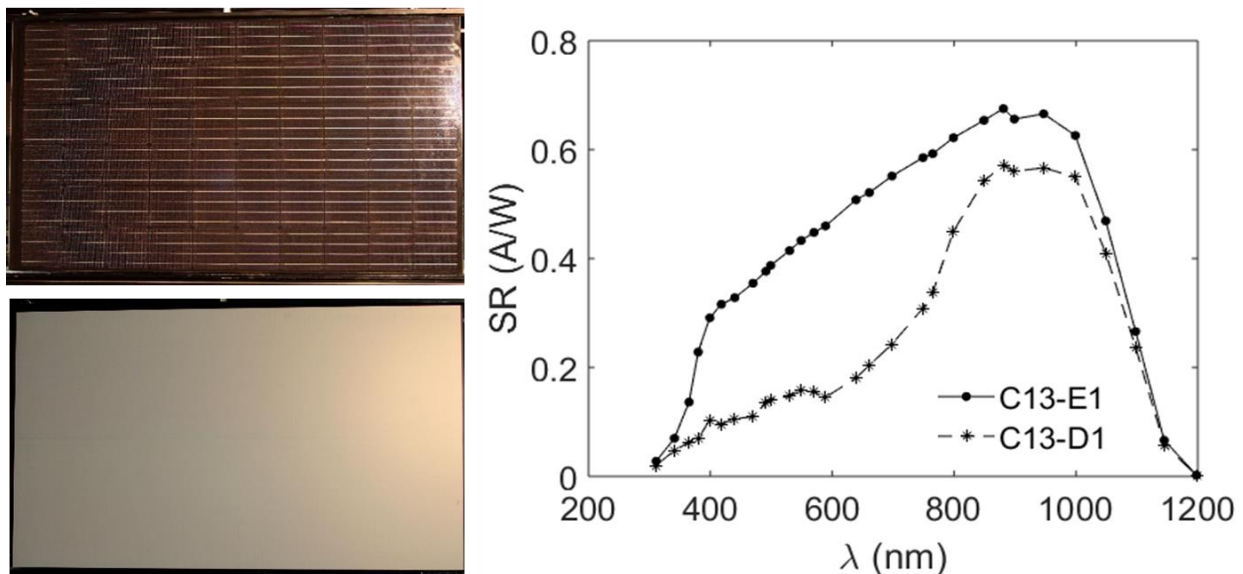
Figure 20: Example of an SR measurement conducted by SUPSI on a white colored PV module.

Improvement of linearity measurements for solar modules

The aim of this objective is to investigate the impact of different irradiance levels on the electrical power output of PV modules manufactured with different technologies and designs.
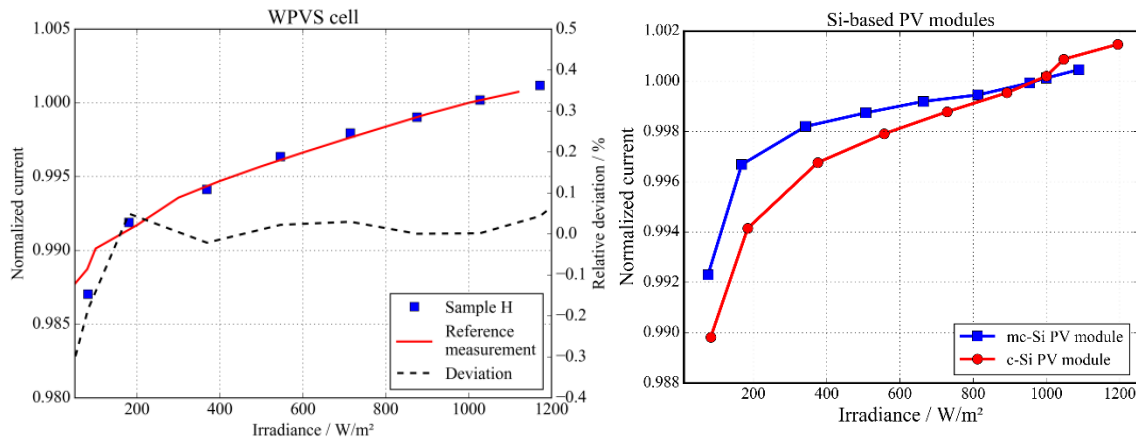

Figure 21: Left side: Non-linearity of a WPVS cell derived with the LED-based solar simulator and compared to our DSR setup for cells. Right side: Non-linearity of two different PV modules.

An LED-based linearity characterization has been developed in combination with the DSR-method and is published in Sträter et al. 2019.With the ability to change the irradiance gradually by modifying the LED current of each LED channel, Figure shows a linearity measurement of a WPVS cell compared with the linearity determined with our conventional DSR measurement setup. The relative deviation accounts to less than 0.1 % for an irradiance of more than 200 W/m². The deviation for lower irradiances can be explained by the irradiance dependent spectral mismatch non-uniformity, as the measured current has not been corrected to demonstrate the effect.

At TUBITAK the linearity characterizations of PV modules manufactured with different technologies were performed according to the IEC 61853-1 and IEC 60904-10 standards. Measurements were performed using a xenon light-based pulse type solar simulator system and a set of 8 different attenuation masks in front of the light source (Figure). Using attenuation masks enables the irradiance of simulator to be adjusted from 1000 W/m² to 100 W/m². Before the measurements, the simulator system at each irradiance level from 1000 W/m² to 100 W/m2 was characterized to determine the effect of spectral match, spatial non-uniformity and temporal instability on electrical parameters (Isc, Voc, Pmax) of PV modules according to the requirements of IEC 60904-9 standard. Linearity measurements were conducted for various module technologies, including mono-Si, poly-Si, CIGS and bifacial modules.
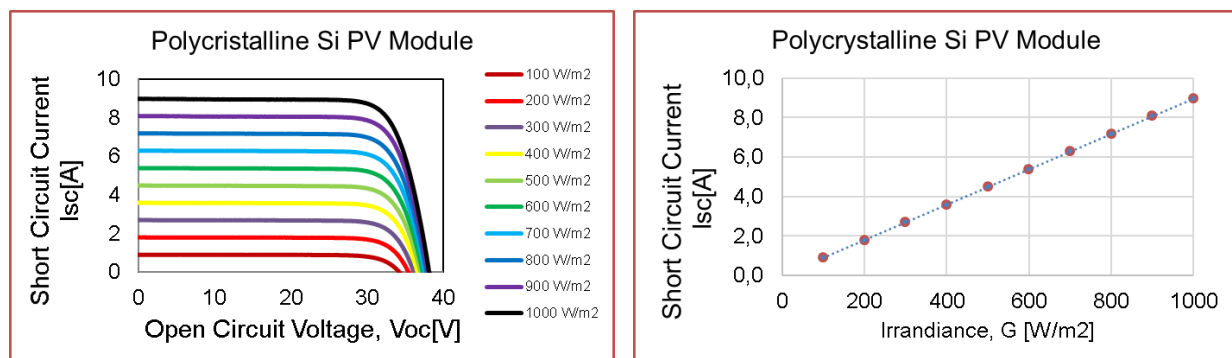

Figure 22: Non-Linearity measurement performed at TUBITAK with attenuation filters.

At NPL a new technique for linearity measurements of PV devices based on digital light processing (DLP) and spatial dithering has been developed. The proposed system utilises a digital micromirror device (DMD) coupled

with projection optics and a high-power LED array, developed in A3.1.3. By creating a series of patterns projected on the device under test with a specific number of bright and dark pixels, linearity measurements can be implemented through a spatial dithering process. Since the dithering process is mechanical, it is expected that any spectral variability effects for the different dithering levels or electrical non-linearities of the light source are avoided. The developed system can provide thousands of measurement points on the linearity curve of a device in seconds, which is impossible with any other currently established methods.
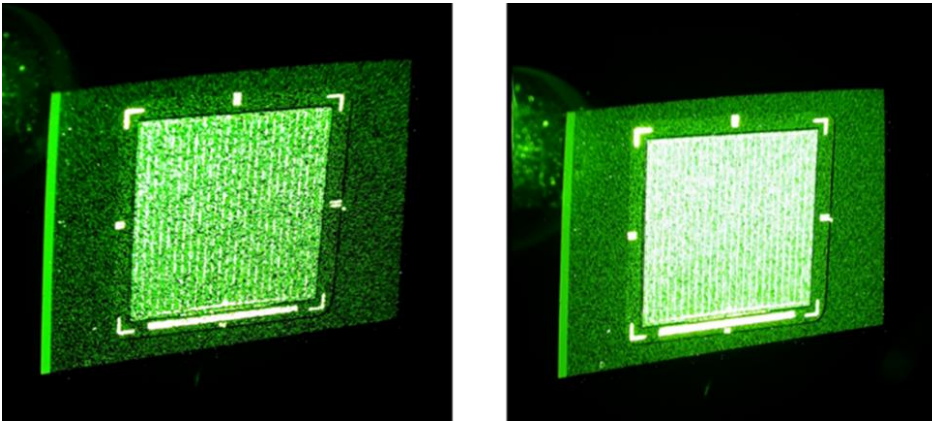

Figure 23: Pictures of a projection pattern on a reference cell, with 30% illumination level on the left and 50% illumination level on the right

Measurements of reference cells provided by PTB are acquired and results are compared with the DSR method at PTB. Results demonstrate that the DLP method provides equal measurement accuracy compared to conventional systems, but at significantly higher resolution (points on the linearity curve) and order of magnitude higher measurement speed. The switching speed of the DMD, which is shorter than 100 µs, allows high speed pattern generation, which applies the different illumination levels. The application of mechanical shading ensures electrical and spectral linearity of the system, for a given system light source, while an arbitrarily large number of illumination levels can be achieved, which provides the high resolution on the linearity curve of a device. Measurements are implemented in seconds, which is orders of magnitude faster than other currently established methods. Measurement results with two different reference cells (RCs), a linear one and a non-linear one is presented in Figure .
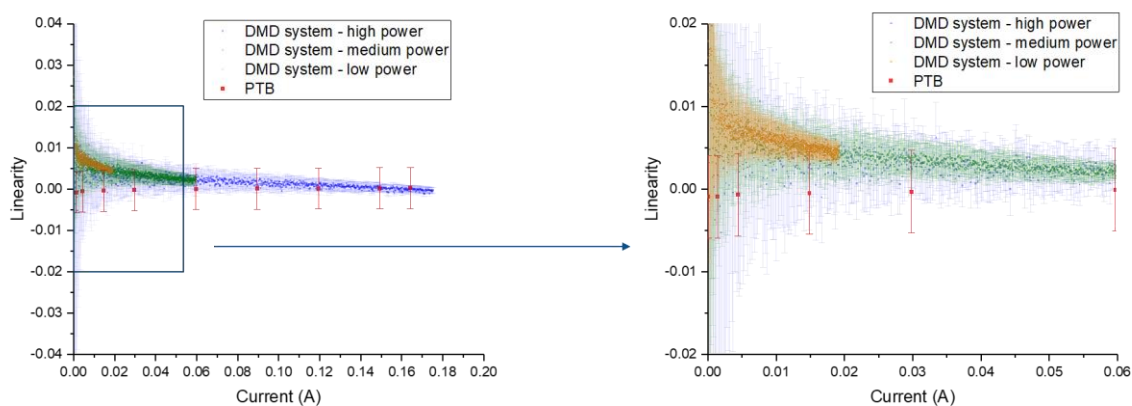

Figure 24: Linearity measurement results using the DLP projection system, for a linear RC (full range on top, zoomed in low light range at bottom graph). Three different power levels have been used (blue, green and orange dots). Measurement results from a DSR system are also included for comparison (red dots). Uncertainty estimations are included in the graphs for all points.
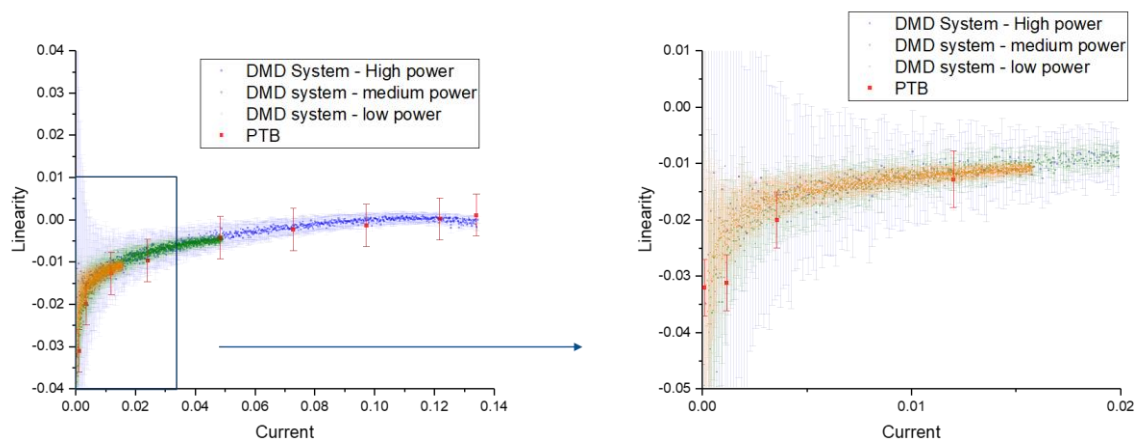
Figure 40: Linearity measurement results using the DLP projection system, for a non-linear RC (full range on top, zoomed in low light range at bottom graph). Three different power levels have been used (blue, green and orange dots). Measurement results from a DSR system are also included for comparison (red dots). Uncertainty estimations are included in the graphs for all points.

For both samples there is good overall agreement between the two methods with some small differences for the linear RC for low light levels (irradiance levels below 100 W/m2), marginally within the uncertainty budget. The differences at low light levels that can be observed for the linear sample in Figure can potentially be due to the different spectral profile of the light sources between the DLP and the DSR system. The results demonstrate that the DLP method using spatial dithering provides equal measurement accuracy compared to conventional systems, achieving a significantly higher number of points on the linearity curve and order of magnitude higher measurement speed, since thousands of points on the curve can be acquired in seconds.

Temporal dithering was also investigated, but tests demonstrated that due to the finite current decay time of any solar cell sample and the DMD's timing limitations, it is not a possible option.

The system overview, the DLP linearity methodology and experimental results were presented in EUVSEC 2020 as an oral presentation. In addition, a manuscript has been submitted to the Measurement Science and Technology Journal (IOP).

Improvement of the Temperature dependence measurements for PV modules

Under outdoor conditions, a PV module will operate at temperatures different to the standard conditions (25 °C) and its performance will vary with temperature. To accurately evaluate the energy produced it is therefore necessary to determine the temperature dependence of the PV module. In the current state-of-the-art module testing (IEC 61215 and IEC 61646) the temperature dependence is usually determined for temperatures from 20 °C to 60 °C. This range is extended from 15 °C to 75 °C in the IEC 61853-1 standard, which aims at energy rating.

The aim of this objective is to determine the temperature coefficients of PV modules in relation to the technologies and design used. In order to cover the required temperature range for PV modules from 15 °C to 75 °C suitable climatic chambers were constructed.

PTB set up a bifacial-ready climate chamber with two fast-opening rolling gates at front- and backside (Figure41). PV modules can be measured inside the chamber between 15 °C and 75 °C with a temperature non-uniformity of +- 2 °C. The rolling gates enable bifacial measurements without accounting multiple reflections while using front- and backside illumination.
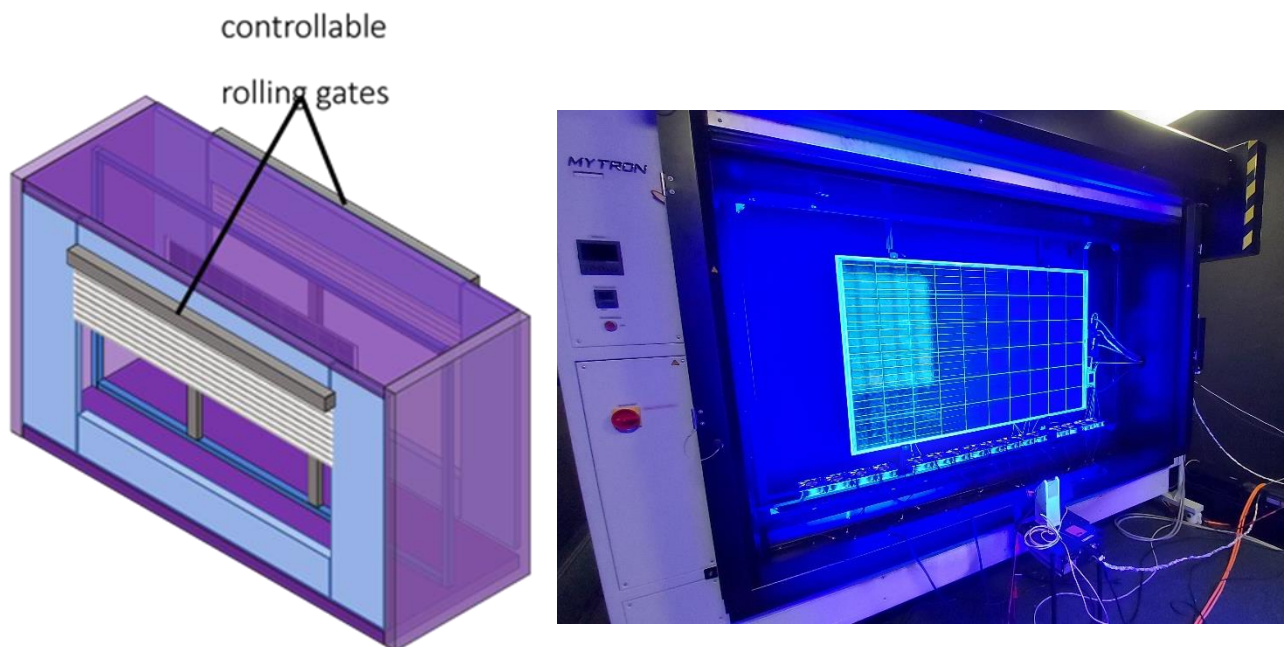

Figure41: Left side: Scheme of the PTB climate chamber. The chamber has two rolling gates at front and back side in order to provide the capability to illuminate bifacial modules simultaneously at front and back side. Right side: Photo of the climate chamber during a measurement.
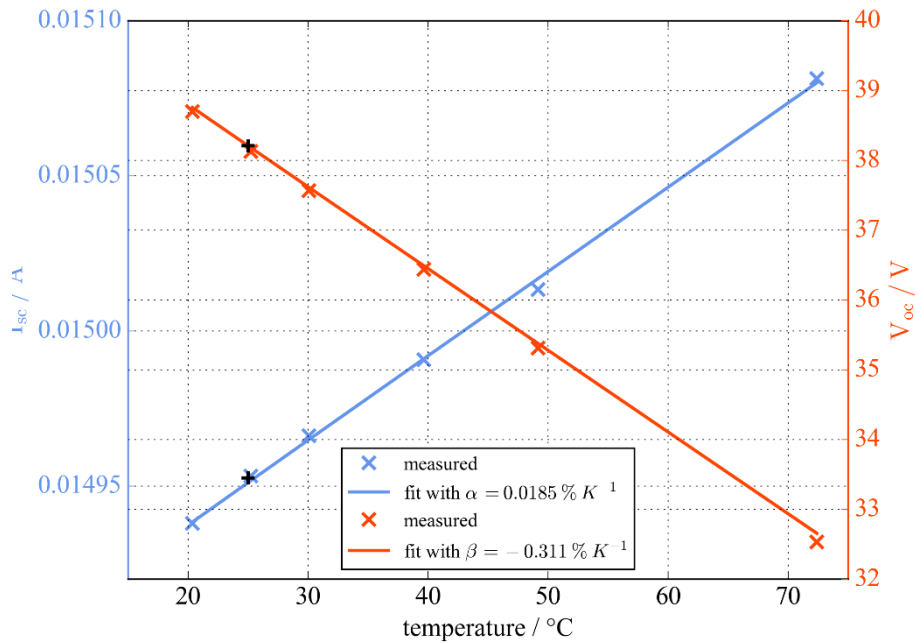
Figure42: Temperature coefficient of a poly-Si-module measured with the LED solar simulator and the setup climate chamber.

At TUBITAK, a climate chamber has been installed into the existing solar simulator setup (Figure 25). The chamber is capable to vary temperature between 15 °C and 75 °C with a temperature non-uniformity of +- 1 °C. An example measurement is shown in Figure 26, where a poly-Si module has been measured with the upgraded setup.

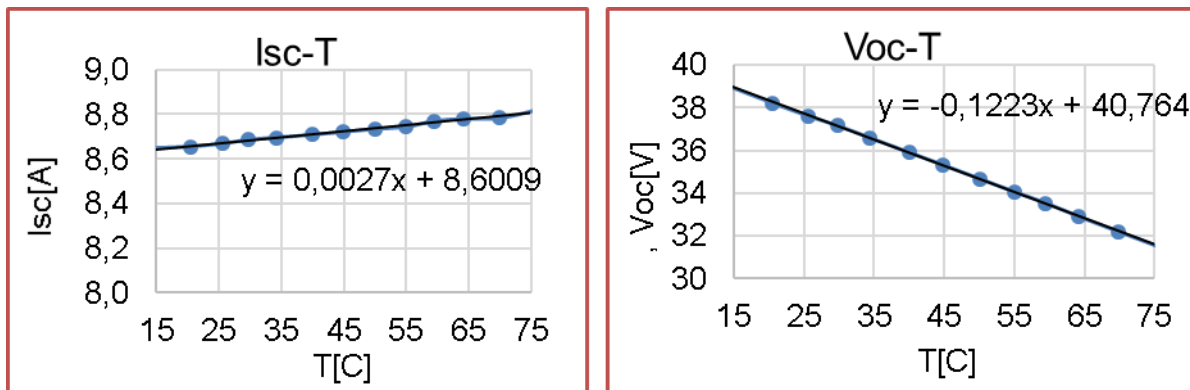Figure 25: Temperature chamber installed at TUBITAK.

Figure 26: Temperature coefficients of a p-Si module measured with the upgraded equipment at TUBITAK.

In order to compare the determination of temperature coefficients between an LED-based setup at PTB and a Xenon-based solar simulator setup at TUBITAK, a bidirectional comparison with a poly-Si module has been carried out. Results of the comparison are shown in

Table . It is apparent, that the alpha coefficient of PTB is slightly smaller compared to TUBITAK. This is probably due to the fact, that the PTB solar simulator provides infrared irradiance only up to 1050 nm. Since the spectral responsivity is temperature-dependent especially in the IR, missing solar simulator irradiance will lead to a lower temperature dependence of the ISC. Compared to the data sheet of the manufacturer, both results in alpha are significantly lower. Since data sheets of poly- and monocrystalline modules of this company state the same temperature coefficients, it is assumed that the mono-Si values were not actually measured by the company but copied from another data sheet.

Table 5: Temperature coefficients for an identical type of mono-Si modules measured by PTB and TUBITAK. In addition, the values given by the company are shown.

Factor	PTB	TUBITAK	Data Sheet
alpha	0.0182 %/K	0.0205 %/K	0.05 %/K
beta	-0.286 %/K	-0.290 %/K	-0.31 %/K
gamma	-0.413 %/K	-0.424 %/K	-0.43 %/K

Improvement of angular dependency measurements for solar modules

The angular dependence is a crucial parameter for the energy rating as most PV installations use a fixed orientation and hence as the sun moves during the day the module is illuminated from a series of angles that all contribute to the overall power generation. The angular dependence of power generation can strongly depend on the technology used (e.g. thin film technologies are believed to perform better at low angles than c-Si) and on the packaging materials used within the module design.

The aim of this objective is to characterise the influence of the relative orientation of the PV module to a collimated light source on its power generation.

PTB developed a measurement technique in order to determine the source-side angular distribution of the light field generated by the LED-based solar simulator By capturing the light field of the simulator with a digital camera and adding coordinates to each pixel, integrating over the photographed scenery provides a radiance distribution that is intercalibrated with a corresponding reference cell measurement. The method is described in detail in Riechelmann 2019. The LED solar proved to have an incidence angle of 15.6°, where 80 % of the irradiance in the test plane originates from (Figure 28).
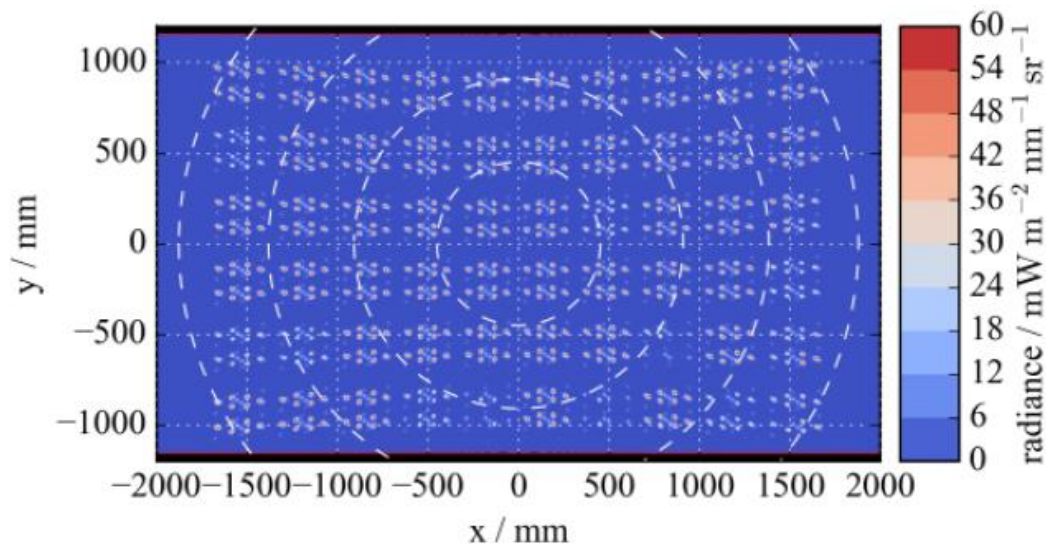

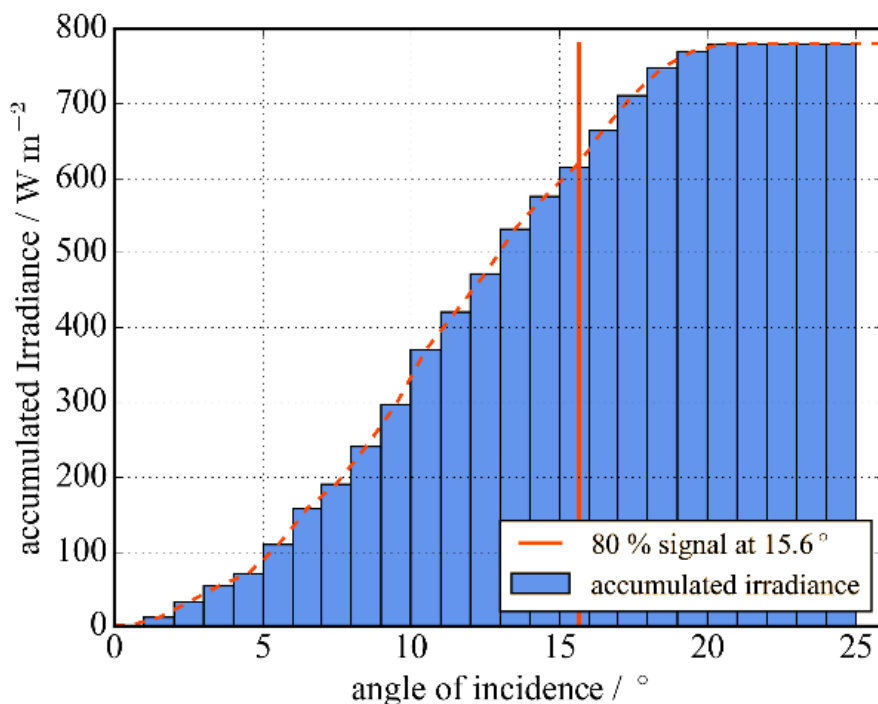Figure 27: Radiance emitted by the LED solar simulator at PTB.

Figure 28: Result of integrating the radiance distribution ring-wise, starting at 0° incidence angle. Most irradiance is originating from an opening angle of 15.6°.
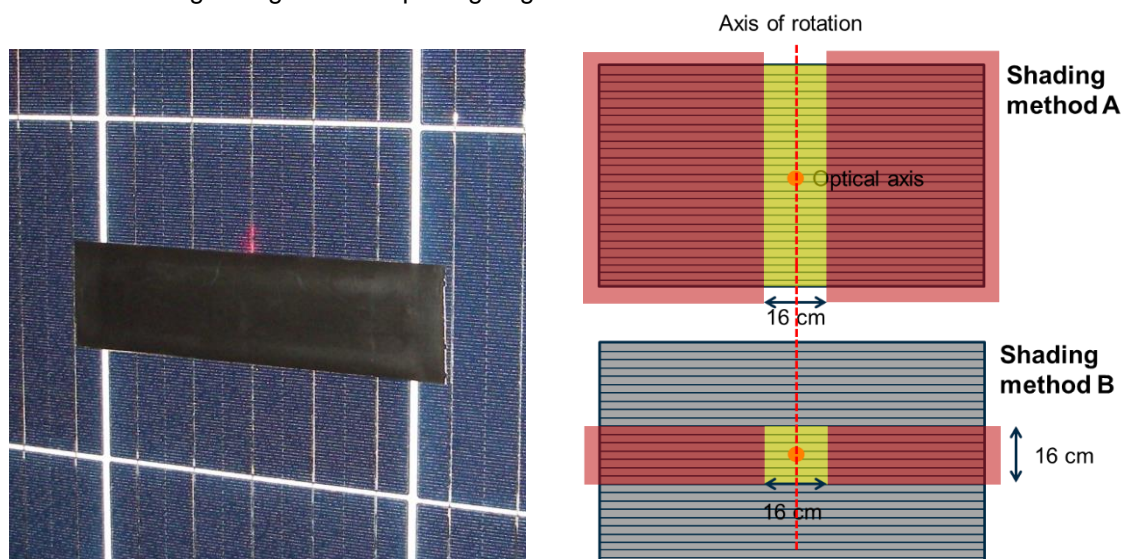

Figure 29: Application of non-destructive angle of incident measurement by shading cells partially. For CIGS and CdTe modules two shading methods are applied (left-hand side) while for poly-Si PV modules only one cell needs to be shaded.

TÜV Rheinland conducted measurements of angular response at PV modules based on a non-destructive procedure based on shading specific cells on the device under test (Figure 29) developed earlier in Herrmann et al. 2014. In a former project c-Si PV modules have been measured with this technique (Herrmann, Schweiger 2017). In this work CIGS and CdTe modules have additionally been evaluated. For all three module technologies the angular responsivity factor ar is calculated according to IEC 61853-2, shown in Table . CIGS and CdTe without anti-reflective coating show slightly higher ar compared to poly-Si, while both poly-Si and CIGS modules with anti-reflective coating show a similar ar factor of 0.144 and 0.146, respectively.

Table 6: Angular responsivity values for different PV module technologies and glass types used. The ar values of all probes with identical technology and glass have been averaged.

Module Type (probes)	Glass Type	Averaged ar
c-Si (11)	floating glass	0.159
c-Si (8)	anti-reflective	0.144
CIGS (2)	floating glass	0.169
CIGS (2)	anti-reflective	0.146
CdTe (2)	Floating glass	0.166

At PTB, we also adapted the method developed by TÜV Rheinland in our LED solar simulator setup. We mounted the module in the 5-axis holder and partially shaded an axis in the middle cell string of the device under test (Figure). Compared to measurement of TÜV, we observed a rise in IAM at angles higher than 80°, which is probably connected to stray light effects due to interreflections between the PV module and its surroundings. Using values below 80° AOI results in a ar factor of 0.161, which is a reasonable value for a PV module with standard floating glass.

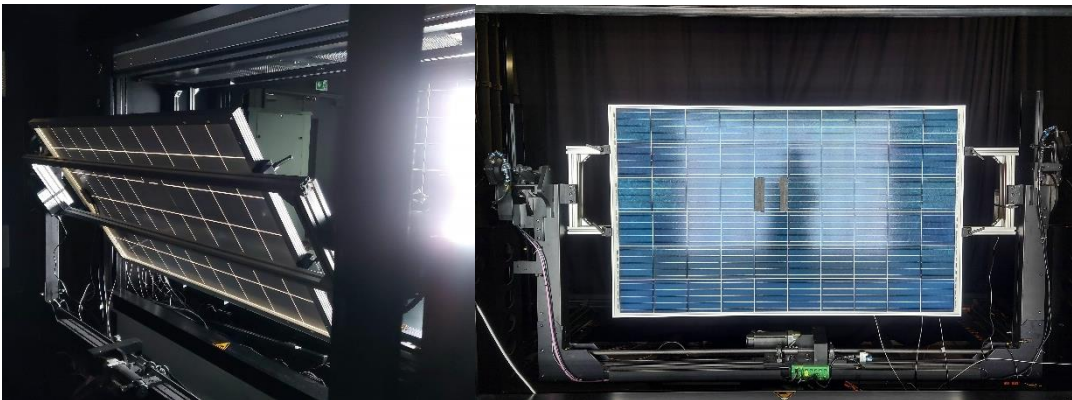
Figure 30: Left-hand side: View on the backside on a mounted PV module during an IAM measurement. Right-hand side frontside of the mounted PV module, the cell shaded for applying the TÜV Rheinland method is placed centrally in the rotating axis of the module holder.
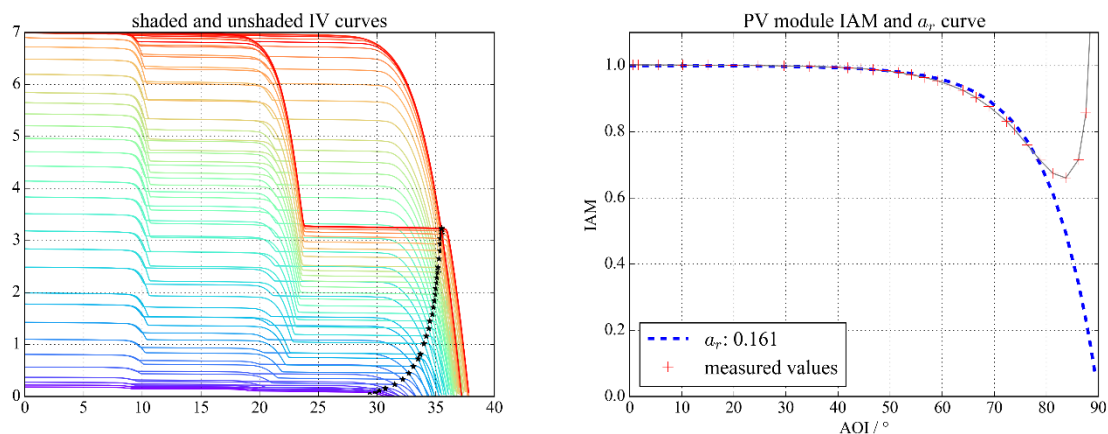

Figure 31: Left-hand side: 34 shaded and 34 unshaded IV curve measurements. The voltage of the unshaded measurement is scaled to 59/60, according to the TÜV Rheinland method. The interception points are marked with a star at each measured angle position. Right-hand side: IAM derived from the shaded Isc values. The ar factor is calculated based on measurements below 80°.

In addition to the TÜV method, PTB evaluated a modification of this method, that allows to skip the proposed unshaded measurements, in order to speed up the measurement process. Therefore, not only the dedicated cell of the module is shaded, but also at least two cells of the both outer cell strings of the module under test (Figure 32). This leads to a suppression of the two outer cell strings 1 and 3, the middle cell string 2 is the only string left contributing to the Isc of the module. This way, no interception point is needed for the determination of the Isc of the shaded cell in cell string 2, the Isc of the module can be used directly. Using the Isc of the module leads to results shown in Figure 32, an ar factor of 0.156 is derived with the modified method, which is a negligible difference to the original TÜV method.

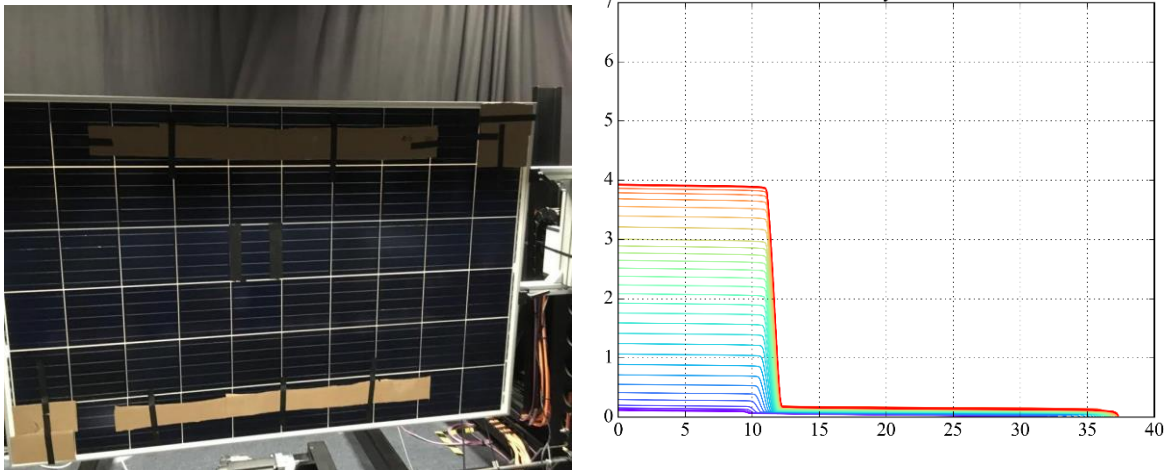Figure 32: Left-hand side: PV module is shaded additionally at the outer cells to suppress contribution from cell string 1 and 3. Right-hand side: corresponding IV curves of the shaded module, the cell string 2 is the only one left substantially contributing to the Isc of the PV module.
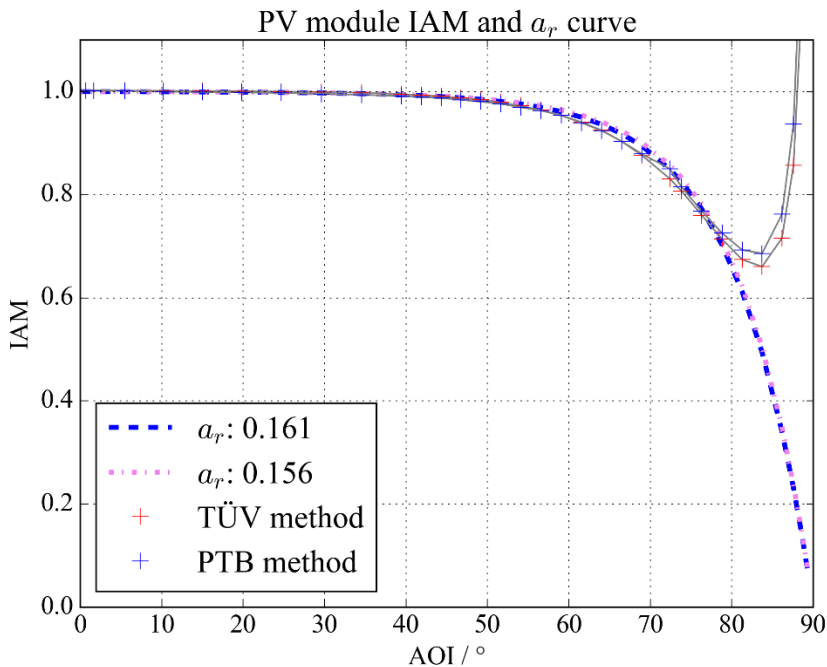

Figure 33: Comparison of original TÜV approach and PTB-modified approach. The differences in determination of the ar factor are negligible.

In order to examine the influence of the spatial distribution on measurement accuracy, we apply an algorithm described in Plag 2019, multiplying the radiance field of the solar simulator with both the PV module and the WPVS cell responsivity, integrating the values and comparing the resulting effective irradiance. Using a WPVS reference cell for the calibration of an s-Si module results in an angular mismatch of about 0.132 % (Figure). We also calculated the difference for a larger reference cell, this results to a smaller angular mismatch of 0.058 %. The irradiance of our solar simulator originates mainly from inside a 16° opening angle (Figure 28) and fortunately reference cells and PV modules only differ slightly in their cosine behavior in this region. For flat-bed simulators, where the light source is very near to the PV module, the situation will be more severe. And should be examined in the future based on the developed algorithms.
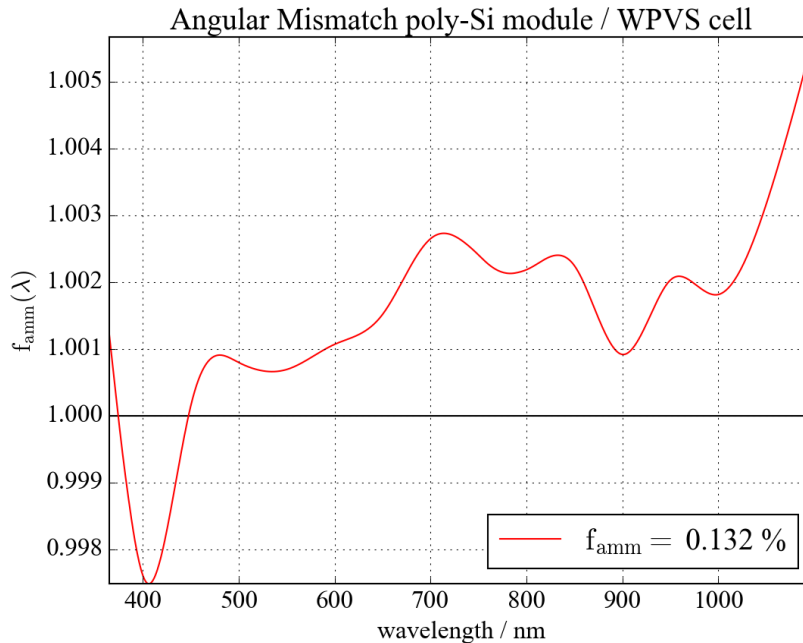

Figure 34: Spectrally resolved angular mismatch between a poly-Si module and a WPVS reference cell.

SUPSI improved its set-up for angular response measurements for cells and applied it to a set of test devices characterized by different antireflective coatings (Pasmans et al. 2019). The measurement uncertainty was recalculated for the new set-up. Figure shows some details of the new measurement set-up together with its measurement uncertainty. SUPSI participated to an international round robin to validate the new set-up. The results of this round robin were presented by N. Riedel at the PVPMC 2019 workshop organized by Sandia National Laboratories.

| Class AAA large area pulsed solar simulator Pasan IIIb | Turn table with device holder and digital goniometer, calibrated reference cell, calibrated temperature sensor | Detail of the turn table with device holder and digital goniometer | Detail of the digital goniometer |
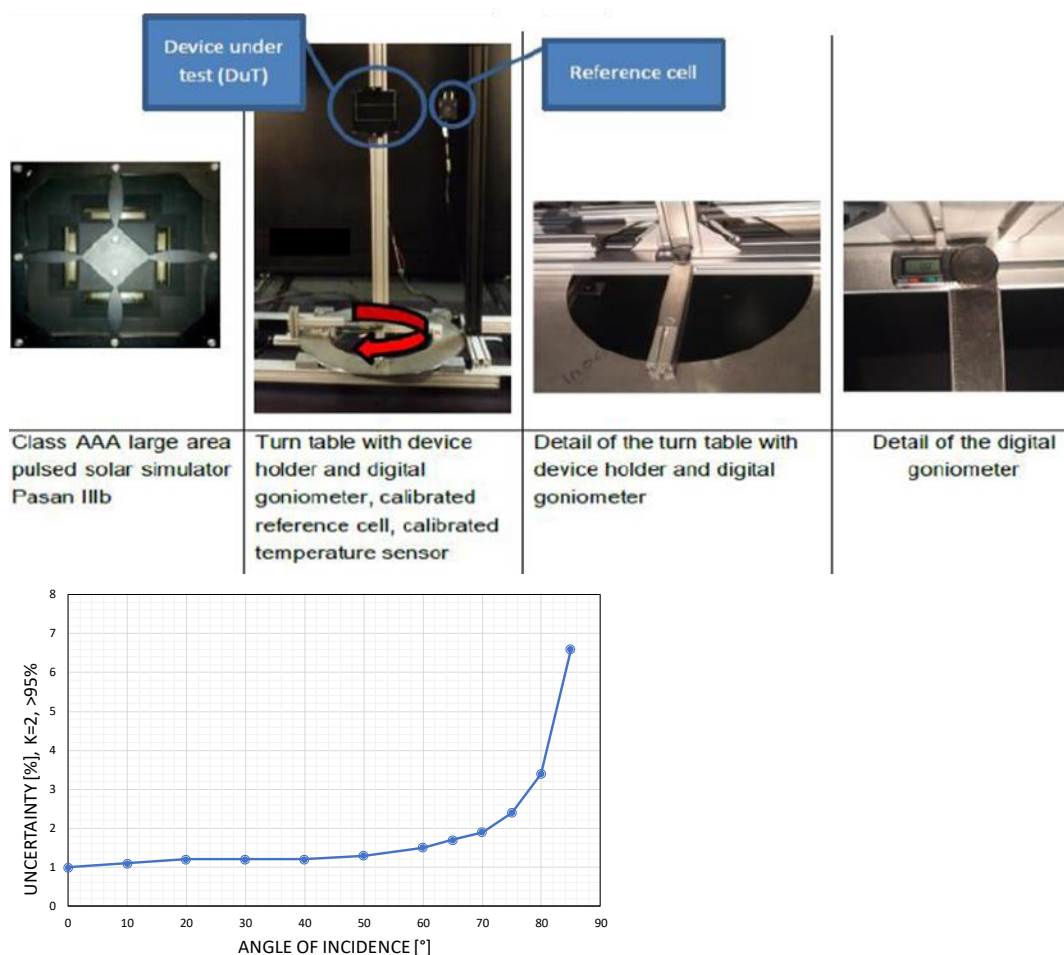
Figure 35: Details of the angular response measurement set-up at SUPSI together with the measurement uncertainty u[%] (k=2).

In a second step SUPSI implemented the non-destructive method developed by Herrmann et al. 2014 for the measurement of full-size modules. The approach was compared to the destructive approach described in the IEC61953-2 standard, where a single cell is contacted through the back of the module. Figure shows the results of this inter-comparison. The difference of the two measurements lies within the calculated measurement uncertainty.

Figure 36: Angular response measurement of a single cell compared to the non-destructive measurement of a full module of same type.
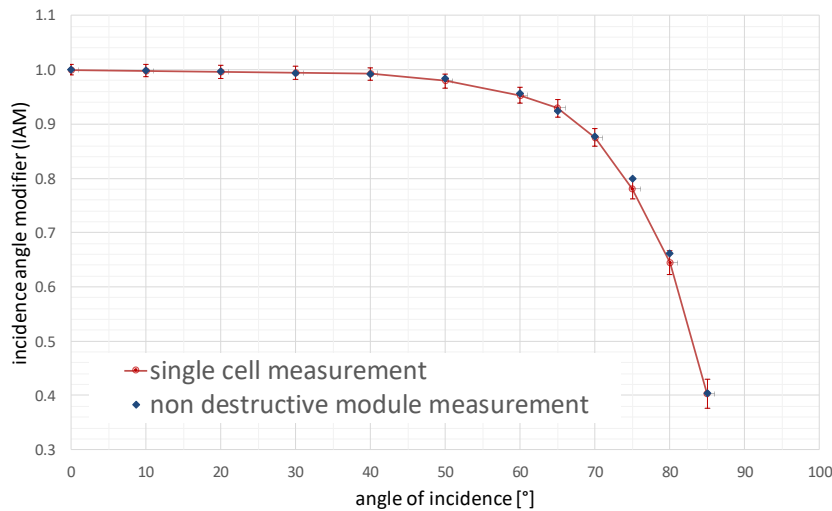
Improvement of nominal operating module temperature measurements for standard solar modules

The efficiency of a solar module depends on its temperature and its temperature depends on the wind. The efficiency of most modules decreases with higher temperature. Thus, solar modules with a good thermal design reach higher yearly energy yield. The outdoor surface temperature of a PV module will at least be the same as the ambient air temperature and will be further heated up by the incident irradiance, however, losses of heat will also occur due to heat conduction, convection, and radiation. The rate of heat convection depends on both the difference in temperature between the PV module and the air surrounding it and the wind speed with respect to the module surface. The major challenge of this objective is to ensure a reproducible wind speed approaching the PV module under test.

At PTB a testing facility for the determination of the nominal module operating temperature (NMOT) has been set up (Figure 55). In the test stand three modules are mounted, surrounded by a surface imitating a larger solar surface. While all modules have temperature-sensors stripped to the outside of their backsheet, the module in the middle has two additional temperature sensors laminated between waver and backsheet. Measurements were performed according to the current Energy Rating standard IEC 61853-2 for about 100 days.
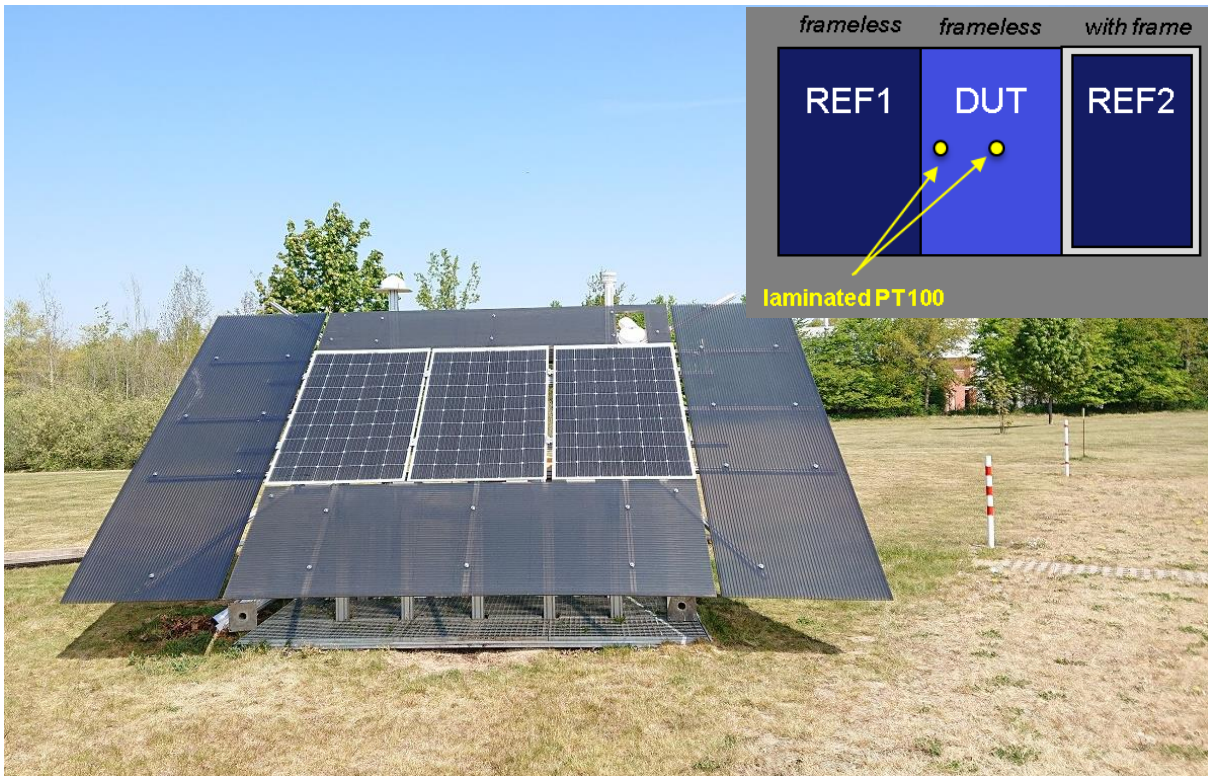
Figure 37: Wind test facility at PTB in Braunschweig, Germany. The legend in the upper right shows the setup of the devices under test. The module in the middle is a frameless c-Si module with two temperature sensors laminated into its interior.

Figure shows the test facility set up by SUPSI in Lugano (Switzerland). The two reference modules on the right are the same type of module as installed at PTB. REF1 is a frameless glass back sheet module, whereas REF2 is the same type of module, but framed. In addition to these SUPSI installed more modules needed also for activity 3.8, including 2 colored modules (white and terracotta) and the same modules without colored glass. 7 months of data were acquired and analyzed within the framework of this project.

Figure 56: Wind test facility at SUPSI in Lugano, Switzerland. The two reference modules used for the inter-comparison with PTB are shown on the right.

To study the reproducibility of the nominal module operating temperature (NMOT) measurement accord. IEC61853-2, PTB and SUPSI compared the wind coefficients of the reference modules measured at their site. Both laboratories implemented the data analysis approach proposed by the IEC standard. To exclude any differences due to the interpretation and/or implementation of the filtering algorithms, an alignment was done on a 1-month data set. After this the data measured in the two locations were processed and compared. Table shows the average and standard deviation of the daily wind coefficients U0, U1 and the NMOT (module temperature calculated for G = 800 W/m2, Tamb = 20 °C and w = 1 m/s) for both locations. Figure shows the two distributions for NMOT. 26 % of data at SUPSI and respectively 41 % at PTB are filtered out by the irradiance and wind filter imposed by the standard. The difference is due to the different meteorological conditions with more cloudy days in Braunschweig.

		SUPSI	PTB	SUPSI 5 min avg	PTB 5 min avg
valid days*/total days		123/166	66/112	123/166	66/122
U0	Avg	36.07	42.46	32.00	35.35
	StDev	2.25	5.08	4.59	9.30
U1	Avg	0.55	0.84	3.88	4.44
	StDev	0.31	0.57	4.10	5.11
NMOT	Avg	41.93	38.71	42.37	40.51
	StDev	1.25	2.09	1.22	3.02

Table 7: Comparison of PTB and SUPSI wind dependence results once calculated with the instantaneous wind speed and once with the 5 minute moving average as defined within the IEC standard.

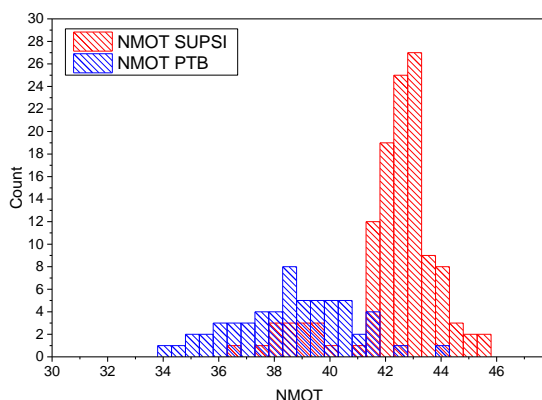* accord. IEC61853-2 filter algorithms

Figure 57: Statistical distribution of the daily NMOT values measured at PTB (Braunschweig/Germany) and SUPSI (Lugano/Switzerland).

The accuracy of the thermal model when applying the measured wind coefficients is here analyzed as well. Differences in U0 and U1 are only significant when they also affect the RMS error of the predicted versus the measured module temperature. Table shows therefore the respective mean bias error (MBE) and random mean square error (RMSE) for module temperature.

An analysis of the deviation observed between SUPSI and PTB showed that the major impact is coming from the very different wind conditions in the two locations and the impact of the surrounding environment (grass/metal lattice bat PTB versus Gravel/concrete grounding at SUPSI). The impact of the NMOT uncertainty on the climatic specific energy rating is however limited as demonstrated in Deliverable 7.

To reduce the measurement uncertainty of the reported data a 10 days average is used and a correction to consider seasonal variations is applied. The last requires the availability of long-term data of the two reference modules. Table shows the results obtained for two different devices under test (DUT) (1 c-Si module with glass/backsheet and 1 c-Si module with glass/glass module) measured at SUPSI from February 2020 to September 2020. In average at SUPSI a full NMOT measurement with 10 valid days required 15 days and in the worst case 30 days. The seasonal corrections were in the range of ±1.2 °C. The requirement of having a range of wind speeds of at least 4 m/s is here neglected as being too restrictive for Lugano, where the wind conditions are much lower as for example in Braunschweig.

		U0 avg10days	U1 avg10days	NMOT avg10days
DUT1 (glass/backsheet)	Avg.	29.84	3.44	44.04
	StDev	0.49 (1.7%)	0.33 (9.6%)	0.25 (0.6%)
DUT (glass/glass)	Avg	31.84	1.86	43.71
	StDev	1.01 (3.2%)	0.82 (44.3%)	0.21 (0.5%)

Table 8: Average and standard deviation of the wind coefficients U0, U1 and NMOT measured at SUPSI for two different c-Si modules (DUT1 and DUT2). The data are based on 102 NMOT measurements with 10 days average each.

Based on the results and experience of this round robin, recommendations have been given to the IEC working group responsible of the revision of the current standard.

Improvement of nominal operating module temperature measurements for emerging solar modules (BIPV modules)

When talking about building integration of PV modules two aspects must be considered, one is the aesthetical integration and the second is the integration of the PV module into the building skin. The first is for example

achieved by changing the color/front appearance of the PV module, whereas either applying standard products to the building (BAPV) or by using PV products which replaces the building components like roof tiles or curtain walls (BIPV). How the NMOT measurement procedure can be applied to these products was here investigated.

In a first step SUPSI analyzed the NMOT data of the 2 colored modules mounted on the test facility shown in Figure and compared the measured NMOT parameters of the colored modules with the one of the same modules without colored glass (Table). Within a former project, the same modules were monitored for over one year for the purpose of energy yield assessments and significant differences in temperature have been observed for both. The NMOT measurements showed a 9 °C lower NMOT for the white module, whereas the red module has a NMOT which is approx. 2°C higher. In general, the U_1 value [W/m^2/°C m/s] which describes the wind dependency, is larger for glass back sheet modules, as are the white and its reference module. The red and its reference modules are instead glass/glass modules which shows to have a lower wind dependency and respectively a lower U_1 value.

Module lable	Avg			StDev		
	U0	U1	NMOT	U0	U1	NMOT
REF white (10 days avg)	**29.84**	**3.44**	**44.04**	*0.49*	*0.33*	*0.25*
white (10 days avg)	49.43	4.25	34.95	*1.99*	*1.12*	*0.39*
REF red (10 days avg)	**31.84**	**1.86**	**43.71**	*1.01*	*0.82*	*0.21*
red (10 days avg)	30.46	1.11	45.43	*1.36*	*1.07*	*0.32*

Table 9: Average and standard deviation of the wind coefficients U0, U1 and NMOT measured for the two colored modules (white and red) and its transparent reference modules (REF white and REF red).

Due to the COVID-19 pandemic it was not possible to apply modifications to the existing NMOT test facility and data from former projects had to be used to analyze the impact of different ventilation conditions from the back. The pictures in Table 10 shows the test facilities analyzed for this purpose.

Solarbrick project • 2014-2018 • 7°inclination/south • open rack vs. fully insulated	**IEA PVPS Task 15 RR** • 2019-2020 • 90°inclination/south • ventilated façade	**PV Construct project** • 2016-2020 • 25°inclination/south • vent. roof vs. fully insul. roof tiles

Table 10: Test facilities used for the determination of NMOT parameters of building integrated modules, with a description of the period of the measurements, the inclination/orientation of the module surface and the investigated mounting conditions.

The main difference lays in the availability of 1-minute resolution data instead of sec resolution data. Before proceeding with the extraction of the NMOT parameters (U_0 and U_1) it was demonstrated that the IEC61853-2 approach can be applied also to higher resolution data when a much longer time frame of minimum 1 year is considered. Beside this it has to be mentioned that the purpose of this analysis was focused on the relative change in the wind coefficients for different system configurations (module back-side ventilation and inclination) and not on the accuracy of the absolute values. The following paragraphs shows the results of the first scenario.

Insulated roof at very low inclination (Solarbrick project)
The insulated modules have an around 20 °C higher NMOT compared to the ventilated modules. The U_1 values of the insulated modules are very low and close to each other independently of the type of the module. In the case of ventilation, the U_1 value of the glass/glass modules is as expected lower than the one of the glass/backsheet module. The glass/glass module NMOT is affected by a higher difference between cell and back off module temperature and is so underestimated when measured by attaching the temperature sensor on the back of the module. In the insulated module this difference is significantly reduced due to the position of the sensors within the sandwich module/insulation material.

Module lable	Avg (2014)			StDev (2014)		
	U0	U1	NMOT	U0	U1	NMOT
ventilated glass/backsheet	**30.78**	**1.93**	**45.31**	*2.84*	*0.46*	*1.67*
insulated glass/backsheet	**18.05**	**0.32**	**64.46**	*1.00*	*0.28*	*1.96*
ventilated glass/glass	**37.93**	**1.47**	**41.04**	*3.73*	*0.77*	*1.59*
Insulated glass/glass	**18.58**	**0.17**	**64.06**	*1.24*	*0.45*	*2.11*

Table 11: Average and standard deviation of daily wind coefficients U0, U1 and NMOT measured for a c-Si glass/glass module and a glass/backsheet module installed at the same inclination (7°) but once fully ventilated (open rack) and once with a 20 cm thick back.

Thermal NMOT parameters of bifacial modules
SUPSI, with support of JRC, defined some preliminary recommendations for the purpose of the NMOT measurements of bifacial modules. Following assumptions are made:

- the same thermal model used to calculate the module temperature of mono-facial module is valid also for bifacial modules, when replacing the irradiance G with the sum of the front G and rear Gr irradiance.

$$T_{mod} = T_{amb} + \frac{G + G_r}{u_0 + u_1 \cdot w}$$

  Note: The validity of this assumption still needs some experimental validation, but it is more accurate than using just front irradiance, because it considers the increase of temperature due to rear irradiance in combination with the bifaciality of the module.

- the standard mounting conditions defined for mono-facial modules (south facing open-rack, tilt=37.5±2.5°, module height=1 m above ground) can be maintained also for bifacial modules, except for the additional requirements for back side-irradiance.

- *Note: The applicability of u0 and u1, measured on a tilted south facing test rack, for the calculation of the CSER of vertical E/W facing modules has still to be verified.*

Taking these assumptions into account, the measurement procedure for the determination of the thermal coefficients (u0, u1) must be adapted in the following parts:

- The non-uniformity on the rear side of the module should be below 10% and it must be measured according IEC 60904-1-2 $6.3.2. "… *besides the reference device used for the irradiance measurement on the rear side, another reference device shall be used to measure the non-uniformity of irradiance on the rear side on at least 5 points. … "*

- Both front (G) and rear irradiance (Gr) should be measured. The rear irradiance sensor should be mounted following the natural sunlight procedure described in IEC 60904-1-2 $5.4.

- To measure the module temperature, the temperature sensors should be positioned in 4 points as defined in the current IEC 61853-2 procedure for mono-facial modules. Even if the temperature sensors are shading the cells, they should be positioned behind the cells. The shading should be limited to a minimum by using appropriate sensors (small size, transparent materials and thin cables). A thermography should be performed before starting with the NMOT measurement to verify the absence of any hot-spot and to verify if the position of the sensor is representative of the average

temperature. If required, the number of sensors can be reduced if it is verified that the average of the measurements is representative of the average module temperature. In general, due to the higher temperature non-uniformity the elimination of one of the measurements for the determination of the average temperature, as done for the mono-facial modules should be omitted. The in average measured non-uniformity should be stated in the report.

- For the <u>fitting of the u0 and u1 thermal coefficients</u>, the sum of the front and rear irradiance (Gr) must be used instead of the only front irradiance G.

PTB, TUBITAK, TÜV Rheinland, SUPSI and LU contributed for this objective that resulted in deliverable D7. For the success of this objective it was required that these and partly other partners of the consortium like JRC or FhG consulted each other and compared the results of their new measurement facilities. For example, PTB provided a special non-linear reference solar cell that was calibrated at PTBs established DSR facility to NPL for the test of their completely new approach for the measurement of the non-linearity of a solar cell. As different partners focussed on different methods and needed the consultation of the others, this objective could not have successful if it would be done by only one individual partner.

PTB, TUBITAK, TÜV Rheinland, SUPSI and LU of this consortium improved and extended their portfolio of calibration methods necessary for Energy Rating concerning GT-Matrix, AOI, NMOT, SR and Non-linearity or a part of it. In the publishable summary a detailed list of the current calibration services provided by the individual members is given.

This objective was successfully achieved.

RMG1:

The aim of the RMG was to study how calibration of photovoltaics is performed, how measurement uncertainty is evaluated for such calibrations, and to get acquainted with current progress regarding standardization of the field, especially energy rating. During the research, the investigation of the current standards and its applicability in practice presented itself as a main task. PTB personnel were providing the researcher with specific guidelines, advice and documents needed for completing the research.

This RMG research was created so it consisted of two main parts. First part was related to review of the progress made thus far in the field of energy rating and calibration of photovoltaics. This included extensive investigation into standardization in this field.

Literature review
The aim of the task was to review work that has been done in the field of calibration of photovoltaic modules and of the relevant standards. The main focus was put on standard IEC 61853-3. This standard describes procedures and calculations which are performed to determine energy rating of photovoltaic modules.
Peer-reviewed papers in the field made up a big part of the review, as the area of calibration of photovoltaics is still on the rise, with new ideas and formulations being presented fairly often.

Evaluation of measurement uncertainty
The aim of this task was to study measurement uncertainty for the calibration of photovoltaics. It was firstly done according to standard test conditions, and then for the energy output according to the energy rating standard IEC 61853.
Within this task, the researcher got acquainted with the LED-based solar simulator. Research was done regarding temperature characterization of a photovoltaic module, and how it influenced the output of the module. The module is placed within a specially designed chamber which heats the module to the necessary temperature. Regarding this, it was attempted to obtain the best possible uniformity when it comes to temperature of the module.
This task was further expanded into participation in the team within PTB researching vagueness of the standard IEC 61853-3. The standard provides mathematical model according to which energy rating of the PV module is assessed. However, it has been shown that there are different ways to interpret the model, which yields different results. This makes for discrepancies, which are needed to be addressed. To this end, an

intercomparison was performed, where different institutions made their calculations, and the results were compared with aim to find the best solution which will be adapted by all participants. The results of the intercomparison were presented at a conference by the coordinator of the intercomparison.

This objective was successfully achieved.

5   Impact

A number of 20 articles including 10 peer-reviewed journal publications have been written in order to disseminate the outputs of the project.

Partners had 38 presentations including 10 poster presentations at international conferences where the project and its preliminary results were presented. The topic of advanced energy rating was presented at a parallel event to the EUPVSEC conference in September 2018. A minimum of 50 attendees were present from PV research and test laboratories, manufacturers of advanced PV and BIPV products, consultancies and software producers. The event was advertised via the EURAMET website.

The E-Learning has been setup by NPL with a training course featuring 9 detailed articles in 3 modules on metrology for energy rating of photovoltaics and has been made public. A link from the PTB hosted project site to the E-learning system of NPL is given. It is intermediate level.

The project homepage has a blog about PV metrology for energy rating with 12 articles. The name of the course is "PV Module Performance Measurements and Energy Rating"

SUPSI carried out a session at the Monitoring and simulation of the performance and reliability of photovoltaics in the built environment training school from 23-26 October 2018. The school focused on the special requirements and challenges of integrating PV into the built environment and grids, with a focus on the determination and prediction of performance and reliability. School trainees (students, researchers, educators and practitioners) participated in expert lectures, interactive seminars and practical courses.

The 80th IEC TC82 WG2- meeting "Solar photovoltaic energy systems - Modules, non-concentrating" with 108 registrations was organised and hosted by PTB. Not only fruitful discussion about the development of international PV standards have taken place, but also the results of the EMPIR project PV-Enerate could be presented during the laboratory tours to the participants, e.g. the LED-based solar simulator with more than 16.000 LEDs of 18 different spectra for accurate solar module calibrations.

TÜV Rheinland hosted the "PV Module Forum" with more than 100 external European participants from industry, that included a full session "Advanced PV Energy Rating" with 5 presentations from the PV-Enerate project.

In addition, the project results were shown at the PTB boost at the Hannover Messe 2019.

Impact on industrial and other user communities

Designers, manufacturers and end users of PV technology will benefit from the capabilities and outputs developed by the project. The extension of the IEC 61853 energy rating standards developed by the project, and the capacity to measure PV devices according to the new standards will benefit industry by enabling a fair and impartial intercomparison between different technologies.

The achieved faster and more accurate characterisation of PV cells and modules will enable manufacturers to better optimise their products for real applications and locations. The provision of accurate measurement data on BIPV and bifacial modules, as well as comprehensive indoor/ outdoor measurement comparisons will benefit the software used for the design and monitoring of PV installations, hence improving the accuracy of energy yield estimates from PV technology. The suggested common data format for module energy rating developed by the project can be implemented into commercial modelling software thus reducing barriers to collecting, sharing and implementing advanced module characterisation data. Uptake of new measurement standards will reduce the uncertainty in energy yield estimates at the planning stage of a PV project, provide technological solutions to reduce the costs of acquiring such data and encourage rapid uptake of energy rating measurements. Finally, customers will benefit from accurate validated energy rating standards and validated software to inform decisions on choice of technology and optimise system design, delivering more clean energy and better return on investment.

Impact on the metrology and scientific communities

New and improved measurement capabilities are available within the NMIs/DIs to support the adoption of the new standard test conditions for bifacial PV devices according to the new IEC 61853 standards. Documented calibration methods for more accurate determination of PV module power output are available. Two organisations have new capability to measure the operating temperature of modules as a function of wind-speed, which is currently a significant source of uncertainty in module energy rating and this will lead to more

accurate determination of the relevant coefficients. Adoption of the common data format for reporting and sharing module energy rating measurements will reduce the complexity and costs for customers of energy rating measurements and lead to more efficient implementation into end users' models. New measurement facilities, such as LED-based spectral responsivity, LED solar simulator and instrumentation for structure light sources will contribute to improved understanding of the properties and loss mechanisms of new solar technologies.

Impact on relevant standards

Recommendations were submitted to project IEC 60904-1-2 on two different methods to extend the standard test conditions (STC) for bifacial solar devices together with a draft annex providing guidelines for the measurements of bifacial modules required for the energy rating standard IEC 61853. Guidelines on extending the energy rating model and reference conditions to include bifacial PV and PV on buildings were presented during a IEC TC 82 WG 2 meeting and a written technical report distributed afterwards. In the report the required extension of IEC 61853-3 & -4 was demonstrated. It could be shown that the reproducibility of the nominal operation module temperature (NOMT) measurement method described in IEC 61853-2 and required by IEC 61215 is a significant source of uncertainty in predicting the energy yield of PV modules. A member of the consortium took over the leadership in the IEC TC 82 standardisation project for an amendment proposed to IEC 61853-2.

Longer-term economic, social and environmental impacts

To achieve the target, increase in photovoltaics as a source of electricity requires a large Europe-wide increase of PV installations by several 100 GW, with an associated investment cost of several 100 billion Euro. Thus, every percent measurement uncertainty in energy yield estimation leads to a financial uncertainty of several billion Euros. The techniques and standards developed in the project will enable a more precise classification of the expected energy output from different emerging PV technologies such as building-applied and building-integrated PV, based on realistic operational conditions. This will enable, for example, a seamless integration into smart grids through the accurate calculation of the power contribution dependent on the time of day and weather conditions, providing better security of supply. It will also enable more reliable requirements for power control, reducing balance-of-system costs and, most importantly, enable a much-improved forecasting of solar yield. Without the latter, significant percentages of generated electricity may be lost as the distribution infrastructure is not in a state to accept injection from this energy source and it is instead dumped to ensure stability of the power network.

6   List of publications

[1] G. Koutsourakis, M. Bliss, T.R. Betts, R. Gottschalg, Utilising Digital Light Processing and Compressed Sensing for Photocurrent Mapping of Encapsulated Photovoltaic Modules. *Proceedings of EUPVSEC* (2018), https://doi.org/10.4229/35thEUPVSEC20182018-5BO.11.6 https://zenodo.org/record/4055644#.X3HNZWhKi70

[2] R. P. Kenny, E. Garcia Menendez, J. Lopez-Garcia, B. Haile, Characterizing the operating conditions of bifacial modules. *AIP Conference Proceedings 1999, 020014 (2018)* (2018), https://doi.org/10.1063/1.5049253 https://aip.scitation.org/doi/10.1063/1.5049253

[3] J. Lopez-Garcia, A. Casado, T. Sample, Electrical performance of bifacial silicon PV modules under different indoor mounting configurations affecting the rear reflected irradiance. *Solar Energy*. **177**, 471–482 (2019), https://doi.org/10.1016/j.solener.2018.11.051

[4] E. Salis *et al.,* Results of four European round-robins on short-circuit current temperature coefficient measurements of photovoltaic devices of different size. *Solar Energy*. **179**, 424–436 (2019), https://doi.org/10.1016/j.solener.2018.10.051 https://dspace.lboro.ac.uk/dspace-jspui/handle/2134/34784

[5] G. Koutsourakis, M. Bliss, T.R. Betts, R. Gottschalg, Accessing the Performance of Individual Cells of Fully Encapsulated PV Modules Using a Commercial Digital Light Processing Projector. *PVSAT proceedings* (2018), http://dx.doi.org/10.1109/JPHOTOV.2019.2933190

[6] H. Baumgartner, B. Oksanen, P. Kärhä, E. Ikonen, Optical Characterization of III-V Multijunction Solar Cells for Temperature-Independent Band Gap Features. *IEEE Journal of Photovoltaics*. **9**, 1631–1636 (2019), https://doi.org/10.1109/JPHOTOV.2019.2933190

[7] J. C. Blakesley *et al.,* Accuracy, cost and sensitivity analysis of PV energy rating. *Solar Energy*. **203**, 91–100 (2020), https://doi.org/10.1016/j.solener.2020.03.088

[8] P. Kärhä *et al.,* Measurement setup for differential spectral responsivity of solar cells. *Optical Review* (2020), https://doi.org/10.1007/s10043-020-00584-x

[9] C. Schinke, M. Franke, K. Bothe, S. Nevas, Implementation and uncertainty evaluation of spectral stray light correction by Zong's method. *Applied Optics.* **58**, 9998 (2019), https://doi.org/10.1364/AO.58.009998

[10] G. Koutsourakis, J. C. Blakesley, F. A. Castro, Signal Amplification Gains of Compressive Sampling for Photocurrent Response Mapping of Optoelectronic Devices. *Sensors.* **19**, 2870 (2019), https://doi.org/10.3390/s19132870

[11] F. Bausi, G. Koutsourakis, J. C. Blakesley, F. A. Castro, High-speed digital light source photocurrent mapping system. *Measurement Science and Technology.* **30**, 95902 (2019), https://doi.org/10.1088/1361-6501/ab1f40

[12] C. Schinke *et al.,* Calibrating spectrometers for measurements of the spectral irradiance caused by solar radiation. Metrologia (2020), https://doi.org/10.1088/1681-7575/abafc5

[13] F. Plag, PhD thesis, Integral methods of measurement for photovoltaics. *TU Braunschweig,* https://doi.org/10.7795/110.20200615

[14] Sträter, Hendrik; Riechelmann, Stefan; Neuberger, Frank; Winter, Stefan, LED-Based Differential Spectral Responsivity Measurements of PV Modules. *https://www.eupvsec-proceedings.com/proceedings* (2019) https://zenodo.org/record/3784708

[15] S. Riechelmann, Characterizing the Angular Distribution of an LED-Based Solar Simulator for PV Modules. *https://www.eupvsec-proceedings.com/proceedings* (2019) https://zenodo.org/record/3784748

[16] S. Riechelmann, H. Straeter, S. Winter, Determination of a PV module power matrix with an LED solar simulator. *EUPVSEC-proceedings* (2020) https://zenodo.org/record/4049818

[17] J. C. Blakesley, G. Koutsourakis, Energy Rating for Evaluating Performance of Perovskite and Perovskite-on-Silicon Tandem Devices in Real-World Conditions. *Proceedings of EUPVSEC (*2019), http://doi.org/10.4229/EUPVSEC20192019-3CO.6.2 https://zenodo.org/record/4055579#.X3HLCGhKi70

[18] G. Koutsourakis *et al.*, Results of the Bifacial PV Cells and PV Modules Power Measurement Round Robin Activity of the PV-Enerate Project. *Proceedings of EUPVSEC* (2020), http://doi.org/10.4229/EUPVSEC20202020-4CO.2.2 https://zenodo.org/record/4055707#.X3Hc1WhKi70

[19] J. C. Blakesley *et al.*, Effective Spectral Albedo from Satellite Data for Bifacial Gain Calculations of PV Systems. *Proceedings of EUPVSEC* (2020), http://doi.org/10.4229/EUPVSEC20202020-5CO.9.3 https://zenodo.org/record/4055920#.X3HfPGhKi70

[20] G. Koutsourakis, T. D. Eales, I. Kroeger, J. Blakesley, High resolution linearity measurements of photovoltaic devices using digital light processing projection. *Measurement Science and Technology* (2021), https://doi.org/10.1088/1361-6501/abe162 https://iopscience.iop.org/article/10.1088/1361-6501/abe162/meta

This list is also available here: https://www.euramet.org/repository/research-publications-repository-link/

7 Contact details

JRP-Coordinator:

Name:	Dr. Stefan Winter, PTB
Tel:	+49 531 592-4500
E-mail:	Stefan.Winter@ptb.de
JRP website address:	https://pv-enerate.ptb.de